



## Models and analysis of dynamic interaction between aircraft/pilot and ground reactions

W.W.M. Heesbeen, H.T.H. van der Zee (NLR), V.F. Bragazin, V.A. Chochiev, D.S. Emelianov, N.G. Khayrullin, V.V. Strelkov, E.V. Varyukhina, L.E. Zaichik (TsAGI)

Short abstract: Future Sky Safety is a Joint Research Programme (JRP) on Safety, initiated by EREA, the association of European Research Establishments in Aeronautics. The Programme contains two streams of activities: 1) coordination of the safety research programmes of the EREA institutes and 2) collaborative research projects on European safety priorities.

This deliverable is produced by the Project P3 *Solutions for Runway Excursions*. The main objective of this deliverable is to assess shortcomings in current methods and models for analysing aircraft ground control.

---

<b>Programme Manager</b>	M.A. Piers , NLR
<b>Operations Manager</b>	L.J.P. Speijker, NLR
<b>Project Manager (P3)</b>	G.W.H. van Es, NLR

---

<b>Grant Agreement No.</b>	640597
<b>Document Identification</b>	D3.12
<b>Status</b>	Approved
<b>Version</b>	2.0
<b>Classification</b>	Public

**Project:** Solutions for Runway Excursions  
**Reference ID:** FSS\_P3\_NLR\_D3.12  
**Classification:** Public



*This page is intentionally left blank*

## Contributing partners

Company	Name
NLR	W.W.M. Heesbeen
NLR	H.T.H. van der Zee
TsAGI	V.F. Bragazin
TsAGI	V.A. Chochiev
TsAGI	D.S. Emelianov
TsAGI	N.G. Khayrullin
TsAGI	V.V. Strelkov
TsAGI	E.V. Varyukhina
TsAGI	L.E. Zaichik

## Document Change Log

Version	Issue Date	Remarks
1.0	29-01-2019	First formal release
2.0	11-03-2019	Second formal release

## Approval status

Prepared by:	Company	Role	Date
W.W.M. Heesbeen	NLR	Main Author	10-12-2018
V.V. Strelkov	TsAGI	Main Author	17-08-2018
Checked by:	Company	Role	Date
P.J. van der Geest	NLR	Quality Assurance	19-12-2018
Approved by:	Company	Role	Date
G.W.H. van Es	NLR	Project Manager (P3)	29-01-2019
L.J.P. Speijker	NLR	Operations Manager	11-03-2019

## Acronyms

Acronym	Definition
AGL	Above Ground Level
AOM	Aircraft Operating Manual
ATIS	Automatic terminal information service
CACM	Control algorithm of the cockpit motion
CG	Center of Gravity
CS	Certification Specifications
CS-AWO	Certification Specifications for All Weather Operations
C/L	Centreline
EASA	European Aviation Safety Agency
ECEF	Earth Centered of Earth Fixed
EMAS	Engineering Materials Arresting System
FAA	Federal Aviation Administration
FAS	Final Approach Speed
FAVT	The Federal Agency for Air Transport (Rosaviatsiya)
FCOM	Flight crew operation manual
FMS	Flight Management System
FSS	Future Sky Safety
GLONASS	Global Navigation Satellite System
GPA	Glide Path Angle
GPS	Global Positioning System
GRACE	Generic Research Aircraft Cockpit Environment
IAS	Indicated Airspeed
ILS	Instrument Landing System
ISA	International Standard Atmosphere
LG	Landing gear
LNAV	Lateral Navigation
MAC	Mean Aerodynamic Chord
METAR	Meteorological Aerodrome Report
MTOW	Maximum takeoff weight

<b>NLR</b>	Netherlands Aerospace Centre
<b>NPA</b>	Notices of Proposed Amendment
<b>PLA</b>	Power Lever Angle
<b>RCAM</b>	Runway Condition Assessment Matrix
<b>RMS</b>	Root-mean-square
<b>ROPS</b>	Runway Overrun Prevention System
<b>SOP</b>	Standard operation procedures
<b>TALPA</b>	Takeoff and Landing Performance Assessment
<b>TsAGI</b>	The Central Aerohydrodynamic Institute
<b>T/R</b>	Thrust Reverser
<b>VNAV</b>	Vertical Navigation
<b>VREF</b>	Reference Speed
<b>WCF</b>	Wind Correction Factor
<b>WOW</b>	Weight on Wheels

## EXECUTIVE SUMMARY

### Problem Area

Accident and incident data on runway excursions show that the combination of a slippery runway and crosswind significantly increases the likelihood of a veer-off. Pilot guidance material provided by aircraft manufacturers concerning recommended crosswind limits on slippery runways is often based on simplified simulation models. Flight testing on slippery runways under crosswind conditions is usually not performed for safety reasons, and is not required as part of the aircraft certification regulations. Therefore, widespread use is made of ground-based simulation models to assess the ground directional control characteristics under crosswind conditions. Previous research has shown that the basis of a representative simulation of the ground-roll lies in the mathematical model which accurately describes the ground control elements and their mutual interaction. The behaviour of the aircraft on the ground is greatly affected by the ground reaction forces acting on the tyres, and the transmission of these forces through the landing gear to the airframe.

Within Future Sky Safety P3 Solutions for runway excursions, a literature study has been conducted on methods and models for analysing aircraft ground control, particularly in crosswind conditions and on slippery runways. The aim of this study was to identify the shortcomings of these models and explore the areas of improvement [1]. The current report presents the results of follow-up activities, on models and analysis for dynamic interaction between aircraft/pilot and ground reactions. This work concerns an assessment of the potential impact that the identified shortcomings have on the validity of guidance material provided by aircraft manufacturers for crosswind landings.

### Description of Work

To assess the impact of some of the potential shortcoming identified in the literature study, simulator experiments and fast-time simulations have been performed. For the simulations the Fokker 100 model available at NLR has been expanded and employed in different modelling configurations and environmental conditions. Additionally, TsAGI conducted an investigation into the significance of providing load factors information from viewpoint of accuracy of pilot-in-the-loop simulation.

### Results & Conclusions

The results from NLR's simulator experiments and fast-time simulations show there is a significant difference between the maximum crosswind that is considered acceptable by pilots in terms of controllability demands and the crosswind that actually exceeds the capacity of the aircraft to counter the side forces generated by the crosswind in the landing roll. The first leads to significantly lower crosswind limits and is the primary factor in the determination of these limits. Furthermore the results indicate that the amount of turbulence and the sophistication of the landing gear model used in the simulations have an impact on the maximum crosswind the pilot/aircraft can handle. In the derivation of guidance material on crosswind limits by aircraft manufacturers, these aspects should therefore be taken into account.

As it was cleared up by TsAGI's computational research, there exists no essential dependency of the spectrums of load factors during ground run on the type of runway contaminant. Pilot-in-the-loop simulation of landing with using simulator with movable cockpit reveals no dependence of pilot's control quality and accuracy on presence or absence of movability.

## Applicability

The results from this study can be used in future efforts to improve methods for analysing aircraft ground control on slippery runways under crosswind so that more consistent and accurate crosswind guidance material can be developed by aircraft manufacturers.

*This page is intentionally left blank*

## TABLE OF CONTENTS

Contributing partners	3
Document Change Log	3
Approval status	3
Acronyms	4
<b>Executive Summary</b>	<b>6</b>
Problem Area	6
Description of Work	6
Results & Conclusions	6
Applicability	7
Table of Contents	9
<b>List of Figures</b>	<b>10</b>
<b>List of Tables</b>	<b>12</b>
<b>1 Introduction</b>	<b>13</b>
1.1. The Programme	13
1.2. Project context	13
1.3. Research objectives	14
1.4. Approach	14
1.5. Structure of the document	15
<b>2 Analysis of impact of shortcomings in existing models</b>	<b>16</b>
2.1. Introduction	16
2.2. Model Description	16
2.3. Simulator Experiments	23
2.4. Fast-Time Simulations	37
2.5. Conclusions	51
<b>3 significance of providing load factors information</b>	<b>52</b>
3.1. Introduction	52
3.2. Development of the model of forces and moments affecting the aircraft motion under conditions of strong crosswind and various types of runway contamination	52
3.3. Simulation of take off and landing run	60
3.4. Conclusions	69
4 conclusions and recommendations	70
5 References	71

## LIST OF FIGURES

FIGURE 2-1: WIND PROFILE WITHOUT TURBULENCE .....	20
FIGURE 2-2: WIND PROFILE WITH MODERATE NLR TURBULENCE .....	21
FIGURE 2-3: WIND PROFILE WITH MODERATE DRYDEN TURBULENCE .....	21
FIGURE 2-4: WIND PROFILE WITH FADE-IN OF TURBULENCE .....	22
FIGURE 2-5: MAXIMUM FRICTION COEFFICIENT CURVES.....	23
FIGURE 2-6: GRACE – OUTSIDE AND FOKKER 100 COCKPIT CONFIGURATION .....	24
FIGURE 2-7: THE NASA COOPER-HARPER RATING SCALE.....	27
FIGURE 2-8: FINAL APPROACH AND LANDING ROLL - NO TURBULENCE - 4 RUNWAY CONDITIONS - CROSSWINDS BETWEEN 20 AND 35KTS .....	31
FIGURE 2-9: RUDDER ACTIVITY DURING APPROACH AND LANDING ROLL WITH MODERATE AND NO TURBULENCE.....	33
FIGURE 2-10: FINAL APPROACH AND LANDING ROLL - MODERATE TURBULENCE - 4 RUNWAY CONDITIONS - CROSSWINDS BETWEEN 20 AND 35KTS.....	34
FIGURE 2-11: FINAL APPROACH AND LANDING ROLL - 25KTS CROSSWIND - 4 TURBULENCE LEVELS - VARIOUS RUNWAY CONDITIONS .....	36
FIGURE 2-12: LONGITUDINAL CONTROL IN THE BASELINE SCENARIO (40KTS CROSSWIND, DRY RUNWAY).....	40
FIGURE 2-13: LATERAL CONTROL IN THE BASELINE SCENARIO (40KTS CROSSWIND, DRY RUNWAY) .....	41
FIGURE 2-14: DIRECTIONAL CONTROL IN THE BASELINE SCENARIO (40KTS CROSSWIND, DRY RUNWAY) .....	41
FIGURE 2-15: LONGITUDINAL CONTROL IN SEVERE DRYDEN TURBULENCE (20KTS CROSSWIND, ICY (DRY ICE) RUNWAY) .....	42
FIGURE 2-16: LATERAL CONTROL IN SEVERE DRYDEN TURBULENCE (20KTS CROSSWIND, ICY (DRY ICE) RUNWAY) .....	42
FIGURE 2-17: DIRECTIONAL CONTROL IN SEVERE DRYDEN TURBULENCE (20KTS CROSSWIND, ICY (DRY ICE) RUNWAY) .....	43
FIGURE 2-18: COMPARISON BETWEEN SIMULATOR AND FAST-TIME - 25KTS CROSSWIND - DRY RUNWAY - NO TURBULENCE.....	44
FIGURE 2-19: COMPARISON BETWEEN SIMULATOR AND FAST-TIME - 25KTS CROSSWIND - CONTAMINATED RUNWAY - NO TURBULENCE.....	45
FIGURE 2-20: COMPARISON BETWEEN SIMULATOR AND FAST-TIME - 25KTS CROSSWIND - CONTAMINATED RUNWAY - SEVERE DRYDEN TURBULENCE .....	45
FIGURE 2-21: MAXIMUM DEVIATION FROM THE CENTRELINE FOR VARIOUS CROSSWIND AND RUNWAY CONDITIONS (BASELINE SCENARIO AND MODELLING CONFIGURATION).....	46
FIGURE 2-22: MAXIMUM DEVIATION FROM THE CENTRELINE FOR VARIOUS CROSSWIND AND RUNWAY CONDITIONS USING THE GENERIC LANDING GEAR MODEL .....	48
FIGURE 2-23: MAXIMUM DEVIATION FROM THE CENTRELINE FOR VARIOUS CROSSWIND AND RUNWAY CONDITIONS IN LIGHT NLR TURBULENCE .....	48
FIGURE 2-24: MAXIMUM DEVIATION FROM THE CENTRELINE FOR VARIOUS CROSSWIND AND RUNWAY CONDITIONS IN SEVERE NLR TURBULENCE .....	49
FIGURE 2-25: MAXIMUM DEVIATION FROM THE CENTRELINE FOR VARIOUS CROSSWIND AND RUNWAY CONDITIONS IN LIGHT DRYDEN TURBULENCE.....	49
FIGURE 2-26: MAXIMUM DEVIATION FROM THE CENTRELINE FOR VARIOUS CROSSWIND AND RUNWAY CONDITIONS IN SEVERE DRYDEN TURBULENCE.....	50

FIGURE 2-27: MAXIMUM DEVIATION FROM THE CENTRELINE FOR VARIOUS CROSSWIND AND RUNWAY CONDITIONS IN THE BASELINE SCENARIO SIMULATED AT 600Hz .....	50
FIGURE 3-1: CIRCLE DIAGRAM OF SIDE FORCE VERSUS SIDESLIP ANGLE DEPENDENCY .....	53
FIGURE 3-2: CIRCLE DIAGRAM OF ROLL MOMENT VERSUS SIDESLIP ANGLE DEPENDENCY .....	53
FIGURE 3-3: CIRCLE DIAGRAM OF YAW MOMENT VERSUS SIDESLIP ANGLE DEPENDENCY .....	54
FIGURE 3-4: CIRCLE DIAGRAM OF RUDDER EFFICIENCY AS TO SIDE FORCE .....	54
FIGURE 3-5: CIRCLE DIAGRAM OF RUDDER EFFICIENCY AS TO ROLL MOMENT .....	55
FIGURE 3-6: CIRCLE DIAGRAM OF RUDDER EFFICIENCY AS TO YAW MOMENT .....	55
FIGURE 3-7: DIAGRAM OF PNEUMATICS.....	56
FIGURE 3-8: DIAGRAM OF SHOCK ABSORBERS .....	57
FIGURE 3-9: MZ0B VERSUS PK DEPENDENCY.....	58
FIGURE 3-10: SIMULINK DIAGRAM OF THE MODEL OF LANDING GEAR OF TYPICAL COMMERCIAL AIRLINER.....	59
FIGURE 3-11: THE TYPICAL EXAMPLE OF LONGITUDINAL LOAD FACTOR “NX” SPECTRUM.....	61
FIGURE 3-12: THE TYPICAL EXAMPLE OF LATERAL LOAD FACTOR “Nz” AND RUDDER PEDALS “X <sub>H</sub> ” DEFLECTION SPECTRA .....	62
FIGURE 3-13: DESIGN OF “PSPK-102” SIMULATOR .....	63
FIGURE 3-14: INTERIOR OF “PSPK-102” SIMULATOR CABIN .....	63
FIGURE 3-15: COMPARISON OF YAW ANGULAR RATE VARIATION IN THE COCKPIT AND COMING FROM MATHEMATIC MODEL ...	65
FIGURE 3-16: CLASSIFICATION OF “p”, “q”, “r” RELATIVE ANGULAR RATE VALUES .....	65
FIGURE 3-17: THE EXAMPLE OF COINCIDENCE OF LONGITUDINAL LOAD FACTOR .....	66
FIGURE 3-18: BANK ANGLE TIME HISTORY .....	66
FIGURE 3-19: EXAMPLE OF COINCIDENCE OF LATERAL LOAD FACTOR .....	66
FIGURE 3-20: RMS DEVIATIONS OF LATERAL LOAD FACTOR “Nz” WITHOUT USING OF SIMULATOR MOVABILITY .....	67
FIGURE 3-21: RMS DEVIATIONS OF LATERAL LOAD FACTOR “Nz” WITH USING OF SIMULATOR MOVABILITY .....	68
FIGURE 3-22: DEPENDENCY OF LATERAL LOAD FACTOR ON CROSSWIND SPEED FOR VARIOUS FRICTION COEFFICIENTS .....	68

## LIST OF TABLES

TABLE 2-1: TURBULENCE LEVELS FOR LOW ALTITUDE.....	19
TABLE 2-2: FIRST PART OF SIMULATOR EXPERIMENTS .....	24
TABLE 2-3: SECOND PART OF SIMULATOR EXPERIMENTS.....	25
TABLE 2-4: THIRD PART OF SIMULATOR EXPERIMENTS .....	25
TABLE 2-5: THE SIMULATOR EXPERIMENT MATRIX .....	25
TABLE 2-6: EXPERIMENT MATRIX FOR SIMULATOR SESSION C .....	26
TABLE 2-7: COOPER-HARPER RATINGS FROM THE SIMULATOR EXPERIMENTS.....	28
TABLE 2-8: AVERAGE COOPER-HARPER RATINGS FOR EACH SIMULATOR SCENARIO .....	28
TABLE 2-9: CROSSWIND LIMITS BASED ON AVERAGE COOPER-HARPER RATINGS FROM THE EXPERIMENT (INCLUDING MODERATE TURBULENCE) .....	29
TABLE 2-10: MAXIMUM WIND COMPONENTS (INCL. GUSTS) FOR MANUAL LANDINGS (RUNWAY WIDTH 45M OR MORE).....	29
TABLE 2-11: CORRELATION OF RUNWAY CONDITION TO BRAKING ACTION FOR THE SPEED RANGE ENCOUNTERED IN THIS STUDY (BELOW 120KTS) .....	30
TABLE 2-12: INPUT PARAMETERS AND (INITIAL) CONDITIONS FOR THE BASELINE SCENARIO .....	37
TABLE 2-13: TEST MATRIX.....	38
TABLE 2-14: MODELLING CONFIGURATIONS .....	39
TABLE 3-1: MAXIMUM VALUES OF AVAILABLE DISPLACEMENTS, VELOCITIES AND ACCELERATIONS.....	64

## 1 INTRODUCTION

### 1.1. The Programme

FUTURE SKY SAFETY is an EU-funded transport research programme in the field of European aviation safety, with an estimated initial budget of about € 30 million, which brings together 32 European partners to develop new tools and new approaches to aeronautics safety, initially over a four-year period starting in January 2015. The first phase of the Programme research focuses on four main topics:

- Building ultra-resilient vehicles and improving the cabin safety
- Reducing risk of accidents
- Improving processes and technologies to achieve near-total control over the safety risks
- Improving safety performance under unexpected circumstance

The Programme will also help coordinate the research and innovation agendas of several countries and institutions, as well as create synergies with other EU initiatives in the field (e.g. SESAR, Clean Sky 2). Future Sky Safety is set up with expected seven years duration, divided into two phases of which the first one of 4 years has been formally approved. The Programme has started on the 1st of January 2015.

FUTURE SKY SAFETY contributes to the EC Work Programme Topic MG.1.4-2014 Coordinated research and innovation actions targeting the highest levels of safety for European aviation in Call/Area Mobility for Growth – Aviation of Horizon 2020 Societal Challenge Smart, Green and Integrated Transport. FUTURE SKY SAFETY addresses the Safety challenges of the ACARE Strategic Research and Innovation Agenda (SRIA).

### 1.2. Project context

Within the FUTURE SKY SAFETY programme the project *Solutions for runway excursions* (P3) was initiated to tackle the problem of runway excursions. A runway excursion is the event in which an aircraft undershoots, veers off or overruns the runway surface during either take-off or landing. Safety statistics show that runway excursions are the most common type of accident reported annually, in the European region and worldwide. There are approximately two runway excursions each week worldwide. Runway excursions are a persistent problem and their numbers have not decreased in more than 20 years. Runway excursions can result in loss of life and/or damage to aircraft, buildings or other items struck by the aircraft. Excursions are estimated to cost the global industry about \$900M every year. There have also been a number of fatal runway excursion accidents. These facts bring attention to the need to identify measures to prevent runway excursions.

Several studies were conducted on this topic. Most recently a EUROCONTROL sponsored research “Study of Runway Excursions from a European Perspective” showed that the causal and contributory factors leading to a runway excursion were the same in Europe as in other regions of the world. The study findings made extensive use of lessons from more than a thousand accident and incident reports. Those lessons were used to craft the recommendations contained in the European Action Plan for the Prevention of Runway Excursions, which was published in January 2013. This action plan is a deliverable

of the European Aviation Safety Plan, Edition 2011-2014. The European Action Plan for the Prevention of Runway Excursions provides practical recommendations and guidance material to reduce the number of runway excursions in Europe. The Action Plan also identified areas where research is needed to further reduce runway excursion risk. The present project focuses on a number of these identified areas. Four areas of research were selected for which additional research is needed:

1. Research on the flight mechanics of runway ground operations on slippery runways under crosswind conditions;
2. Research on the impact of fluid contaminants of varying depth on aircraft stopping performance;
3. Research on advanced methods for analysis of flight data for runway excursion risk factors, and;
4. Research into new technologies to prevent excursions or the consequences of excursions.

The first research topic is important as accident/incident data on runway excursions show that the combination of a slippery runway and crosswind significantly increases the likelihood of a veer-off. Pilot guidance material provided by aircraft manufacturers for these operations is often based on simplified simulation models. Work Package 3.1 Crosswind and slippery runways of Future Sky Safety identifies the shortcomings of these models and explores the areas of improvement. The objective of this work package is to improve methods for analysing aircraft ground control on slippery runways under crosswind so that more consistent/accurate crosswind guidance material from the manufacturers can be developed.

### 1.3. Research objectives

To assess the impact of some of the potential shortcoming identified in the literature study, simulator experiments and fast-time simulations will be performed. For the simulations, the Fokker 100 model available at NLR will be expanded and employed in different modelling configurations and environmental conditions. Additionally, TsAGI will conduct an investigation into the significance of providing load factors information from the viewpoint of accuracy of pilot-in-the-loop simulation.

### 1.4. Approach

In the first task (*Task 3.1.1: Identification of shortcomings in current modelling in relation to modern aircraft*) of W3.1, a literature study was conducted on methods and models for analysing aircraft ground control. Special attention was given to crosswind and on slippery runways in this literature study [1].

It was shown that pilot guidance material provided by aircraft manufacturers concerning recommended crosswind limits on slippery runways is often based on simplified simulation models. Flight testing on slippery runways under crosswind conditions is usually not performed for safety reasons, and is not required as part of the aircraft certification regulations. Therefore, widespread use is made of ground-based simulation models to assess the ground directional control characteristics under crosswind conditions. Previous research has shown that the basis of a representative simulation of the ground-roll lies in the mathematical model which accurately represents the ground control elements and the interaction between them. The behaviour of the aircraft on the ground is greatly affected by the ground forces acting on the tyres, and the transmission of these forces through the landing gear to the airframe.

The literature study identified several (potential) shortcomings in current methods and models for analysing aircraft ground control [1]. Specifically, concerns have been expressed on the methods used in determining the crosswind guidelines, relating to:

- The use of piloted flight simulator evaluations; and
- The exclusion of gust and turbulence; and
- The use of standard friction values for non-dry runways

Regarding aircraft ground models used to evaluate ground handling in crosswind conditions, the following (potential) shortcomings have been identified in the literature reviewed in this study:

- Over-simplified models for landing gear sub-systems;
- Lack of valid models for extreme conditions, for instance cornering friction values at large yaw angles;
- Inability to simulate local variations, for instance in runway contamination (patches);
- Neglecting the influence of certain runways characteristics like undulations, roughness, and camber;
- Lack of experimental data for the validation of ground handling models; and
- The limited bandwidth of most real-time models.

Some of the concerns mentioned above will be investigated further to assess the potential impact these shortcomings have on the guidance material (crosswind limits) provided by aircraft manufacturers. This will be investigated by conducting simulator experiments and fast-time simulations using the Fokker 100 model available at NLR. By simulating in various (environmental) conditions and (model) configurations, the sensitivity of the ground control behaviour and crosswind limits to these variables will be determined.

The mathematical models of on-the-ground motion of the aircraft developed by TsAGI by that moment [11, 12] are found to be sufficiently detailed and provided acceptable level of convergence of simulation results to flight test data. This study investigates the significance of providing load factors information from viewpoint of accuracy of pilot-in-the-loop simulation. It is well known that for some flight tasks acceleration information provided to the pilot is very important [13, 14, 15, 16, 17]. In this connection it is of interest to evaluate significance of this factor just for conditions of crosswind landing at contaminated runways. In accordance with the pilot's opinion, the type of contaminant affects significantly lateral controllability on runways. But control systems of movability of modern flight simulators do not represent corresponding effects. Thus, useful results may be obtained on this way.

## 1.5. Structure of the document

The structure of this report is as follows:

- Chapter 2 presents the results of the analysis of the potential impact that shortcomings in existing models have on guidance material (crosswind limits) provided by aircraft manufacturers.
- Chapter 3 investigates the significance of providing load factors information.

## 2 ANALYSIS OF IMPACT OF SHORTCOMINGS IN EXISTING MODELS

### 2.1. Introduction

The structure of this chapter is as follows:

- Section 2 describes the simulation model and its different configurations.
- Section 3 describes the setup and results of the simulator experiments and discusses the ratings given by the test pilots on the controllability of the aircraft in different conditions.
- Section 4 describes the setup and results of the fast-time simulations and discusses the effect of different scenarios and configurations on the directional control of the aircraft.
- Section 5 gives the conclusions and recommendations.

### 2.2. Model Description

For this study the Fokker 100 simulation model has been selected because of its high level of fidelity. In this chapter the simulation models will be described and the specific adaptations and variations introduced to this model for this study.

#### 2.2.1. Fokker 100 Aircraft Model

The model definition of the Fokker 100 simulation model [Refs. 2 & 3] and the corresponding data of this model were provided by the Fokker Services company. The simulation model was implemented by NLR in MATLAB-Simulink. The MATLAB-Simulink model is primarily used to perform pilot-in-the-loop simulations on NLR's research flight simulators, GRACE and APERO. However, the model can also be used for desk-top and fast-time simulations.

The Fokker 100 simulation model has been implemented in a modular structure with all the major components of the simulation model as subsystems. This enables the exchange of each standard component with an alternative component that can hold different functionality. The main components include:

- Aerodynamic forces and moments, including stall hysteresis
- Engine forces and moments, including engine dynamics
- Landing gear forces and moments
- Mass properties, total mass and inertia calculations
- Flight Control System, including gearing, deflection limits, trim functions, flaps, speed brake, spoilers, stick shaker and pusher logic

Almost all functions of these components are defined as look-up tables and represent a non-linear simulation model.

Other required functions of the simulation model are provided by generic components with specific Fokker 100 data. These include:

- Atmosphere model including wind and turbulence models

- Landing gear retraction and doors system, nose wheel steering
- Control surface actuator dynamics (no specific F100 data implemented)
- Fuel system
- Avionics, autopilot, autothrottle, FMS, NAV-radios, GPWS, TCAS
- Fokker 100 EFIS cockpit displays and related sensors

The autopilot and autothrottle are generic models and include all standard modes and functionality like LNAV, VNAV, ILS and autoland.

The equations of motion are fully six degree of freedom and use the quaternion equations. Besides the calculation of velocities and accelerations at the centre of gravity the model also transforms these variables to the pilot position in the cockpit. This is required to drive the motion system.

### 2.2.2. Landing Gear Models

One of the variations in the simulation model that has been investigated in this study is the type of landing gear simulation model. Besides the landing gear model defined in the Fokker model definition an alternative, generic, landing gear model has been implemented.

#### **Fokker 100 Landing Gear Model**

The Fokker 100 landing gear model is implemented as described in the Fokker model definition [Ref. 3]. The landing gear is modelled as three struts with each one contact point with the ground. The characteristics of the two tires per strut are accounted for in the model data. Each strut is modelled as a spring and damper system. The specific oleo damper and spring characteristics are defined in the corresponding data tables and also include the characteristics of the tires. The model also contains a fourth contact point for the tail scraper.

Specific features of the Fokker 100 landing gear model are functions for decreasing the maximum side friction with the braking ratio ( $F_{brake}/F_{brake\_max}$ ), and in return also for decreasing the maximum braking friction with the side force ratio ( $F_{side}/F_{side\_max}$ ).

There is no modelling of an actual anti-skid system. The maximum braking data of the model includes the factors for an operational anti-skid system, and therefore this system is always assumed to be active.

#### **Generic Landing Gear Model**

The generic landing gear model has been developed for all types of aircraft and can be configured through its model parameters to match the dimensions and characteristics of the specific aircraft model it is used for. It includes basic calculations for the longitudinal forces, the lateral forces and the normal forces produced by the tires, springs and dampers for each landing gear strut.

The generic model also uses three struts with each one contact point with the ground surface. The struts are modelled as a spring and damper system. The spring and damping characteristics of the tires are included in the data of the strut spring and damper. The model also contains a fourth contact point for the tail scraper.

The main difference between the Fokker 100 and the generic landing gear model are the additional functions for decreasing the maximum side friction with the braking ratio and decreasing the maximum braking friction with the side force ratio. The Fokker 100 model also contains a special lateral slip parameter function that takes into account the cornering power of each individual tire depending on its normal load.

### 2.2.3. Pilot Model

To conduct the fast-time simulations, the Fokker 100 aircraft model needs to be extended with a pilot model that controls the aircraft during the final approach and landing and during the ground roll. Using models developed at NLR in previous studies a pilot model has been constructed that is able to land the aircraft in the conditions (crosswind and turbulence) required for this study.

#### **Airborne Phase**

##### Longitudinal Control

The pilot model controls the aircraft in the longitudinal plane using the *TECS Controller* originally developed at NLR for the AMAAI (Aircraft Models for the Analysis of ADS-B based In-trail following) modelling toolset. It is a generic, integrated autopilot/autothrust model that commands the elevator and thrust to control the longitudinal motion of the aircraft (altitude and speed). It is based on the well-known and well-described Total Energy Concept System (TECS). This concept is aimed at controlling the specific energy rate of the aircraft, which is the sum of the flight path angle and the non-dimensional longitudinal acceleration. The basic principle is that the total energy rate is controlled by increasing or decreasing thrust, whereas the distribution of the energy rate over the two components of the energy rate (flight path angle and acceleration) is controlled by the elevator. This leads to a simple, but very effective, integrated controller that calculates the required thrust and elevator commands.

On top of the basic controller, a number of functions have been added as outer loop control laws, which provide the flight path angle and longitudinal acceleration commands, associated with the selected vertical mode and speed mode. In this study the *Flight Path Angle Hold* vertical mode is used in combination with the *CAS Hold* speed mode.

The parameters for the controller (such as the gains for the inner and outer control laws and the command limits) are identical to the AMAAI implementation. Apart from some modifications to make the AMAAI (3DOF) design suitable for the F-100 model (6DOF), the only change that was made is the addition of pitch damping by feeding back the pitch rate in the inner loop of the elevator control law. The model has not been tuned to accurately reflect realistic pilot behaviour.

The flare is initiated by the pilot model at a specified altitude by commanding a fixed pitch angle of 2.5°, while at the same time retarding the thrust levers to flight idle. The control model used in the flare manoeuvre is based on the pilot model developed at NLR in 2011 to simulate manually flown bailed landings with a Boeing 747.

### Lateral-Directional Control

Lateral-directional control in the airborne phase is based on the pilot model developed for the balked landing study. The pilot model tries to maintain the runway track as closely as possible (track hold mode) using aileron and rudder inputs. The decrab manoeuvre is initiated at a specified altitude. The objective of the decrab manoeuvre is to reduce the crab angle (difference between aircraft heading and track) in order to align the aircraft's longitudinal axis with the runway direction, prior to touchdown. The manoeuvre is determined by a decrab profile (i.e. the magnitude and shape of a sideslip command). The pilot model follows the commanded sideslip angle as closely as possible, by applying the appropriate amount of rudder input. At the same time the pilot model provides roll control (cross-coupling the rudder command to the aileron input), in order to avoid drifting from the runway track.

### **Ground Phase**

After touchdown the thrust reversers are deployed when the weight on wheels switch of the main wheels is triggered, while braking is initiated after ground contact of the nose wheel is detected. Reverse thrust setting (between idle and full) and brake force (between none and full) are applied as specified.

To track the centreline rudder and nose wheel steering are used. The controller that is used in this model commands a heading based on the centreline deviation and its derivative. The error between commanded heading and actual heading is then used with a proportional gain to generate the rudder and nose wheel steering commands. A speed scheduling function reduces the overall gain to 36% below 60kts to compensate for the higher effectiveness of the nose wheel at lower speeds.

### 2.2.4. Wind and Turbulence Models

The wind is simulated using a steady wind profile with a boundary layer function and the addition of turbulence from either the NLR turbulence model or the Dryden turbulence model. These models are described in the following sections. Different levels of turbulence are used for the simulations. The different turbulence levels are listed in Table 2-1.

**Table 2-1: Turbulence Levels for low altitude**

Turbulence Level	Turbulence Intensity	RMS Gust Speed
No turbulence	0	0kts
Light turbulence	0.1	3.0kts
Moderate turbulence	0.2	6.0kts
Heavy turbulence	0.25	7.5kts
Severe turbulence	0.3	9.0kts

## Wind Model

The steady wind profile uses a boundary layer function to account for the reduction of the wind speed close to the ground surface. The reference wind speed is defined at 10m above the ground or runway surface. A surface roughness number determines the shape of the boundary layer function. But in any case the wind speed will be less below the 10m reference height and will be more above this 10m. The shape of the boundary layer can be seen in Figure 2-1.

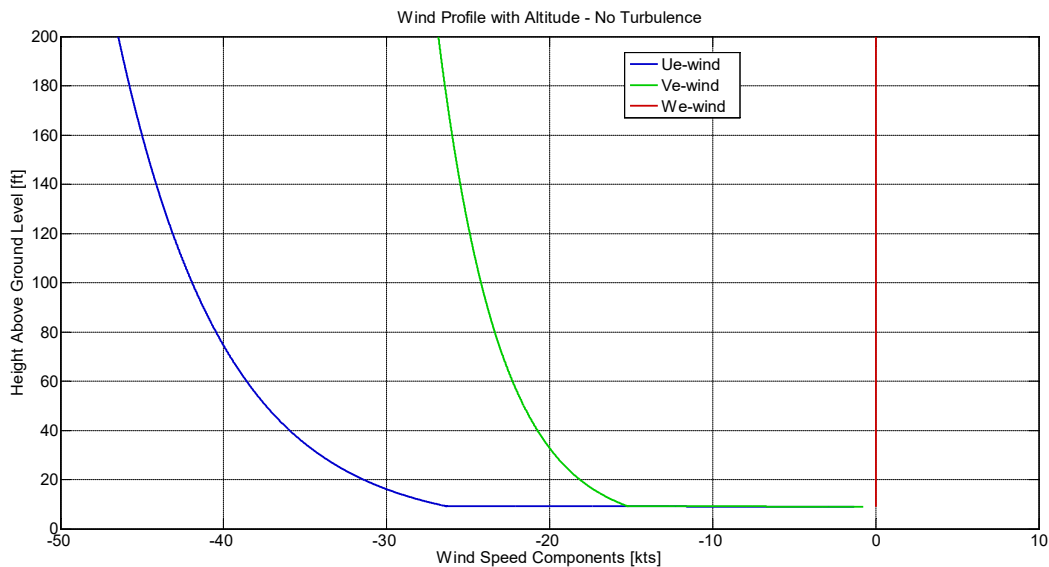


**Figure 2-1: Wind Profile without Turbulence**

To keep the total wind speed constant at 40kts for all scenarios, the wind speed vector is rotated in order to produce the required amount of crosswind on the runway. In Figure 2-1 there is a crosswind of 20kts (at 10 meter above ground) which in this case is equal to the Ve-wind (East) component because the runway heading is due north. At 33ft (10m) height the Ve-wind crosses the 20kts line. The headwind at that point is about 35kts. The Ue and Ve components are faded to zero when the ground speed drops below 40kts to remove unrealistic rolling moments on the aircraft observed in low ground speed and crosswind conditions.

## NLR Gust and Turbulence Model

The NLR gust and turbulence model has been developed to produce more realistic turbulence. The most important feature of this model is the patchiness of the turbulence. This can be observed as an offset in the turbulence for a certain amount of time. This also makes it less predictable than turbulence generated in accordance with the Dryden turbulence model. An example of the wind profile with NLR turbulence as used for this study is presented in Figure 2-2.

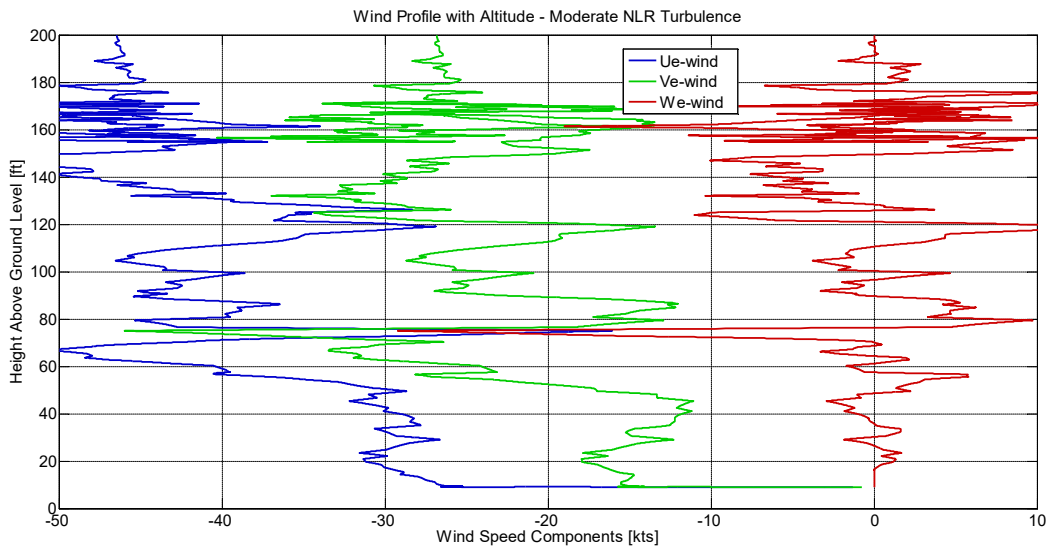


Figure 2-2: Wind Profile with Moderate NLR Turbulence

### Dryden Turbulence Model

The Dryden model is a well-known and widely used turbulence model. This model was selected as a baseline turbulence model. The implementation is taken from the Simulink Aerospace blockset and adapted for use with external inputs for selecting model parameters like the turbulence level. An example of the wind profile with the Dryden turbulence as used for this study is presented in Figure 2-3.

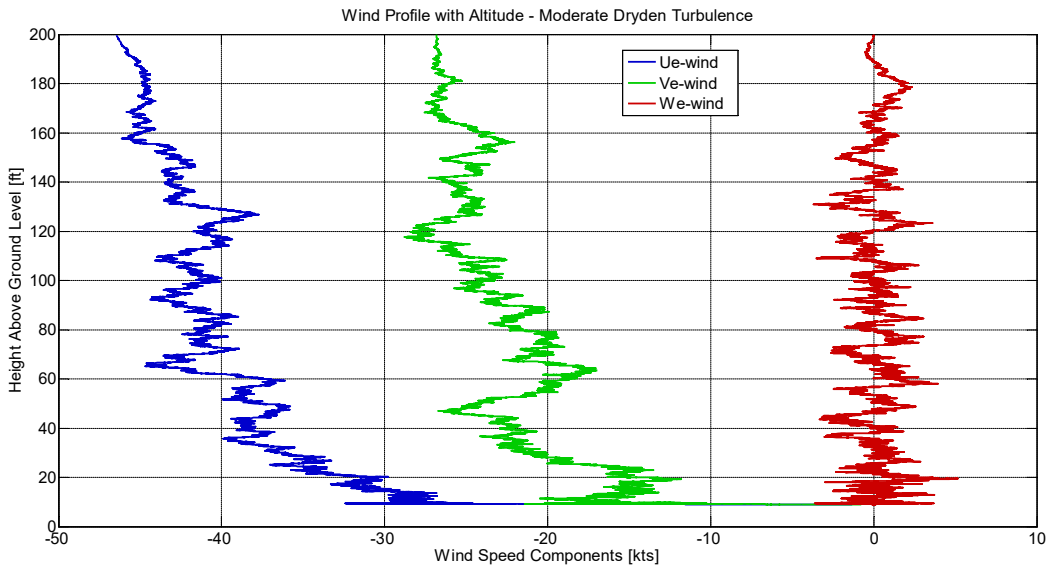
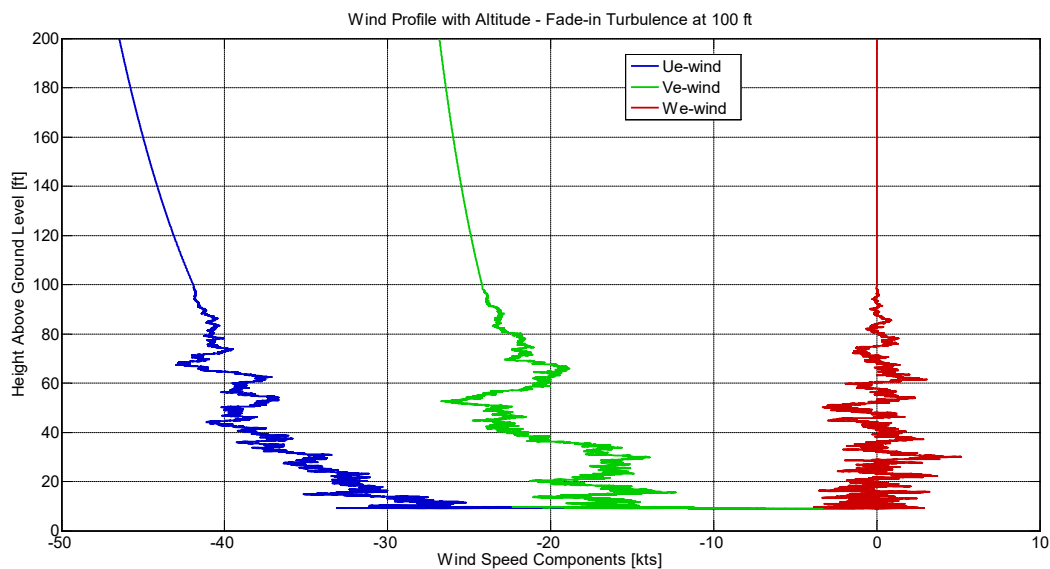


Figure 2-3: Wind Profile with Moderate Dryden Turbulence

For the fast-time simulations a fade-in function was applied to the turbulence. This is done to limit the influence of the turbulence to the interesting part of the approach and landing. Especially at higher levels of turbulence the pilot model can have trouble keeping the aircraft on the glide path and centreline. In extreme cases the aircraft will not land on the runway. To ensure that the aircraft arrives within an acceptable window over the threshold the turbulence is faded-in from 100ft height. See the effect of the fade-in function on the wind profile in Figure 2-4. In this way the turbulence still has influence on the final part of the approach, the landing and landing roll.



**Figure 2-4: Wind Profile with Fade-in of Turbulence**

### Runway Conditions

The Fokker definition contains data for *dry*, *wet* and *icy* runway conditions. The icy condition is in fact a wet or melting ice condition with a very low friction coefficient that is speed dependent at lower speeds. In addition to these three runway conditions, two additional conditions have been added.

The first additional runway condition is the *dry ice* condition. This provides a higher friction coefficient compared to the *melting ice* condition. The dry ice condition is speed independent with a constant friction coefficient. It is based on figures from the Boeing document on aircraft ground performance [Ref. 4].

The second runway condition that has been added is the *contaminated* condition. This condition provides a significant reduction of the friction coefficient with increasing speed. In fact this leads up to the aquaplaning effect at high speeds. The tire slowly starts to float with increasing speed and loses friction. This condition is also based on the Boeing document.

The five runway conditions give a full spectrum of runway conditions for this study. The friction coefficients are depicted in Figure 2-5.

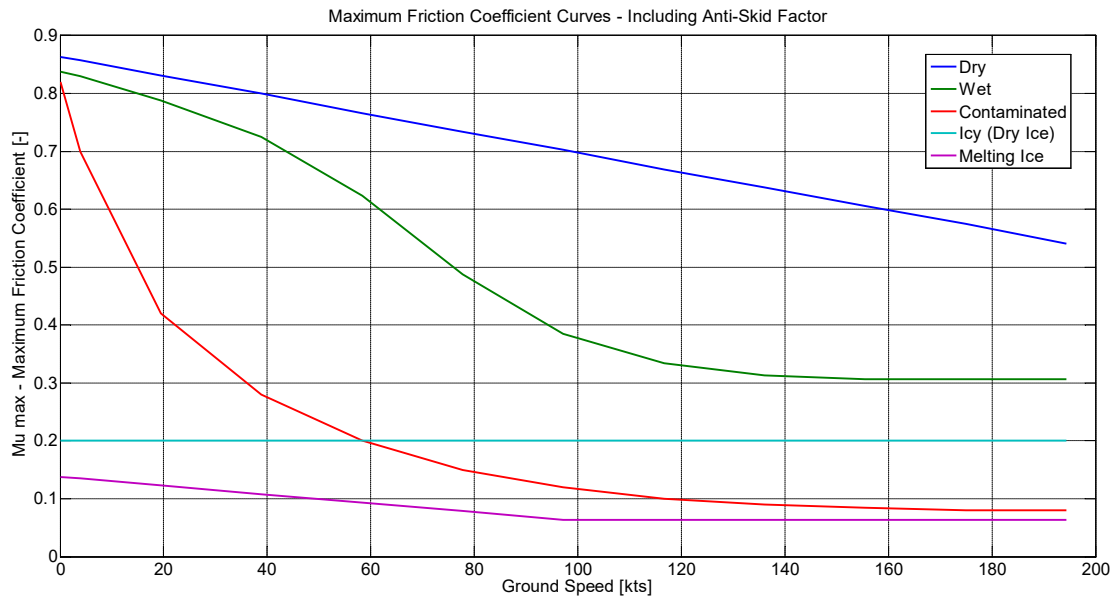


**Figure 2-5: Maximum Friction Coefficient Curves**

### 2.3. Simulator Experiments

The simulator experiments have been conducted to collect pilot ratings on the controllability of the simulated aircraft during the presented scenarios with variations in wind, turbulence and runway conditions. The results from the simulator experiments are also compared with the results from the fast-time simulations. Both simulator experiments and fast-time simulations have been performed with exactly the same aircraft simulation model as well as wind and turbulence models.

#### 2.3.1. GRACE

GRACE is a reconfigurable full flight simulator that is used for all sorts of research projects [Ref. 5]. It can be configured to simulate fly-by-wire aircraft with side sticks like the AIRBUS A320 and A330. It can also be configured to simulate aircraft with conventional controls like the Boeing 747, the Fokker 100 and the Cessna Citation. Figure 2-6 shows the GRACE cockpit in its Fokker 100 configuration including actual Fokker 100 control wheels. GRACE has a 6 degree of freedom electric motion system and a wide collimated visual display system with a field of view of 210 degrees horizontally and 45 degrees vertically. In terms of simulation fidelity it is in the same class as level-D training simulators and very well suited for pilot-in-the-loop evaluations. The motion system can be tuned to optimise the motion cueing for the simulated aircraft and the experiment at hand.



**Figure 2-6: GRACE – Outside and Fokker 100 Cockpit Configuration**

### 2.3.2. Experiment Setup

For this study a small scale pilot-in-the-loop simulator experiment was conducted. During three simulator sessions with three different test pilots a large set of scenarios was tested. All three pilots hold a Fokker 100 currency and they each have more than 1500 hours on this aircraft. A specific test matrix was constructed to assess various influences on landing in crosswind conditions. To limit the number of variations it was decided to only use the Fokker 100 landing gear model and the Dryden turbulence model in the simulator experiment. Variations of the landing gear model and the turbulence model have been assessed in the fast-time simulations.

To focus on different aspects the experiment has been split into three parts. The first part focuses on the effect of crosswind and runway condition in the absence of turbulence. Four runway conditions are combined with four crosswind strengths resulting in 16 combinations.

**Table 2-2: First part of simulator experiments**

Parameter	Values	Variations
Runway conditions	Dry, Wet, Contaminated, Icy (dry ice)	4
Crosswind strength	20, 25, 30, 35kts	4
Turbulence strength	No (fixed)	1

The second part covers an identical test matrix with 16 combinations of crosswind and runway condition but introduces moderate turbulence. The effect of the turbulence can be derived from the differences between the first and second part of the experiment.

**Table 2-3: Second part of simulator experiments**

Parameter	Values	Variations
Runway conditions	Dry, Wet, Contaminated, Icy (dry ice)	4
Crosswind strength	20, 25, 30, 35kts	4
Turbulence strength	Moderate (fixed)	1

The third part focuses on the effect of the turbulence level under different runway conditions. In this case the crosswind strength is fixed to 25kts.

**Table 2-4: Third part of simulator experiments**

Parameter	Values	Variations
Runway conditions	Wet, Contaminated, Icy (dry ice)	3
Crosswind strength	25kts (fixed)	1
Turbulence strength	Light, Moderate, Heavy, Severe	4

This brings the total number of scenarios to 16 + 16 + 12 = 44. The complete simulator experiment matrix is presented in Table 2-5.

**Table 2-5: The simulator experiment matrix**

Experiment Matrix split into 3 parts

TURB	X-WIND	DRY	WET	CONT	ICY
No	20	Scen 1	Scen 5	Scen 9	Scen 13
No	25	Scen 2	Scen 6	Scen 10	Scen 14
No	30	Scen 3	Scen 7	Scen 11	Scen 15
No	35	Scen 4	Scen 8	Scen 12	Scen 16
TURB	X-WIND	DRY	WET	CONT	ICY
Moderate	20	Scen 17	Scen 21	Scen 25	Scen 29
Moderate	25	Scen 18	Scen 22	Scen 26	Scen 30
Moderate	30	Scen 19	Scen 23	Scen 27	Scen 31
Moderate	35	Scen 20	Scen 24	Scen 28	Scen 32
TURB	X-WIND	WET	CONT	ICY	
Light	25	Scen 33	Scen 37	Scen 41	
Moderate	25	Scen 34	Scen 38	Scen 42	
Heavy	25	Scen 35	Scen 39	Scen 43	
Severe	25	Scen 36	Scen 40	Scen 44	

To perform such a large number of runs each run must be as short as practically feasible. Therefore each run starts on short final at an altitude of 500ft. This gives the pilot enough time to get settled on the glide path, get in sync with the crosswind and possible turbulence and finally prepare for the landing. Experience shows that 500ft is sufficient for the pilots to accomplish this.

To be able to compare the simulator results with the fast-time simulations the configuration of the aircraft and the execution of the approach and landing was kept the same as much as possible in both cases. This included performing the rollout with maximum braking and using speed brakes on all approaches. In real-life speed brakes are recommended for landing on contaminated or slippery runways. To keep all approaches comparable in terms of aerodynamic drag it was decided to perform all approaches with the speed brakes extended. Idle reverse was always selected on touchdown and only more than idle reverse was used if the pilot felt this was required for keeping the aircraft under control.

For the third and final simulator session it was decided to look at an additional runway condition. This is the *melting ice* condition. It was interesting to collect also some data on this runway condition in the simulator. In the first part of the experiment this condition was added to the existing four conditions. To limit the amount of additional scenario runs for the pilot, in the second part the dry condition was skipped and in the third part the wet condition was skipped. Therefore the total number of scenarios for this third session was 48. This modified experiment matrix is shown in Table 2-6.

**Table 2-6: Experiment matrix for simulator session C**

Experiment Matrix for simulator session C

TURB	X-WIND	DRY	WET	CONT	ICY	WET ICE
No	20	Scen 1	Scen 5	Scen 9	Scen 13	Scen 17
No	25	Scen 2	Scen 6	Scen 10	Scen 14	Scen 18
No	30	Scen 3	Scen 7	Scen 11	Scen 15	Scen 19
No	35	Scen 4	Scen 8	Scen 12	Scen 16	Scen 20

TURB	X-WIND	WET	CONT	ICY	WET ICE
Moderate	20	Scen 21	Scen 25	Scen 29	Scen 33
Moderate	25	Scen 22	Scen 26	Scen 30	Scen 34
Moderate	30	Scen 23	Scen 27	Scen 31	Scen 35
Moderate	35	Scen 24	Scen 28	Scen 32	Scen 36

TURB	X-WIND	CONT	ICY	WET ICE
Light	25	Scen 37	Scen 41	Scen 45
Moderate	25	Scen 38	Scen 42	Scen 46
Heavy	25	Scen 39	Scen 43	Scen 47
Severe	25	Scen 40	Scen 44	Scen 48

### 2.3.3. Cooper-Harper Ratings

To measure the controllability of the aircraft for the pilot during the different scenarios in the simulator experiments the pilots were asked to rate their effort according to the Cooper-Harper rating scale [Ref. 6]. This is a widely used rating scale for rating the handling qualities of aircraft. Figure 2-7 shows the Cooper-Harper scale with its decision tree diagram. While consulting the Cooper-Harper rating scale the pilots focus on their effort to perform the final approach, landing and rollout. This is the right side of the Cooper-Harper rating scale that quantifies the “Demand on the Pilot in Selected Task or Required Operation”. The left side of the Cooper-Harper rating scale does not apply to this experiment because the aim is not to rate the flight control characteristics of the aircraft.

After completion of each run the pilot would consult the Cooper-Harper rating scale and give the corresponding rating. The ratings of all three sessions are listed in Table 2-7.

Many years of experience with performing pilot-in-the-loop experiments has shown that every pilot has its own personal view on the evaluation of the presented scenarios in the experiment. To get a well-balanced result from a simulator experiment it is preferred to let a large group of pilots participate. For this specific study there were only enough resources to execute a small scale study with three pilots.

To balance out the differences in the personal way of rating the executed scenarios the average of the Cooper-Harper rating is taken for each scenario. These average ratings are presented in Table 2-8.

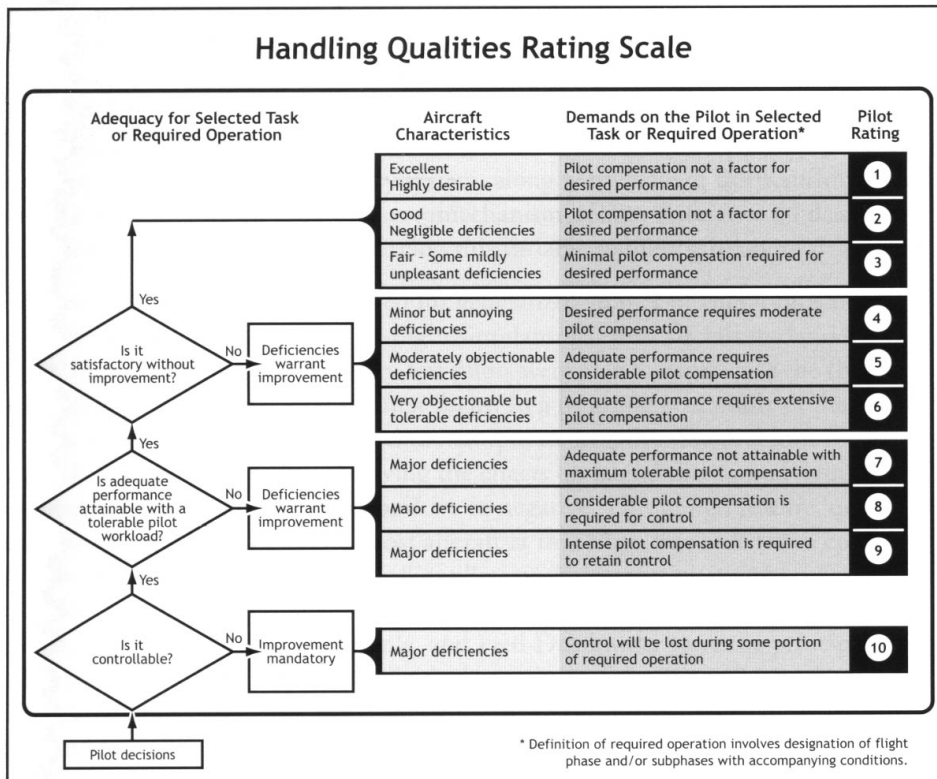


Figure 2-7: The NASA Cooper-Harper rating scale

**Table 2-7: Cooper-Harper ratings from the simulator experiments**

Cooper-Harper ratings for each approach and landing during the simulator experiments, sessions A/B/C

TURB	X-WIND	DRY			WET			CONT			ICY			WET ICE		
		A	B	C	A	B	C	A	B	C	A	B	C	A	B	C
No	20	1	4	3	1	4	2	1	4	2	1	4	3			4
No	25	2	4	3	1	5	2	2	4	3	1	4	4			4
No	30	2	4	3	3	5	3	4	5	5	2	5	5			5
No	35	5	5	5	5	5	3	7	5	5	5	6	6			6
Moderate	20	2	5		2	5	3	4	5	5	3	5	6			4
Moderate	25	3	5		4	6	3	5	5	5	6	5	6			5
Moderate	30	3	6		4	6	4	5	6	4	5	6	4			7
Moderate	35	4	7		5	6	5	6	5	7	6	6	6			5
Light	25							3	5	3	2	4	4			3
Moderate	25							3	5	4	3	5	4			4
Heavy	25							6	6	7	4	5	6			6
Severe	25							6	8		8	8	7			7

**Table 2-8: Average Cooper-Harper ratings for each simulator scenario**

Cooper-Harper ratings average over 3 simulator sessions

TURB	X-WIND	DRY	WET	CONT	ICY	WET ICE
		No	20	2.7	2.3	2.3
No	25	3.0	2.7	3.0	3.0	4.0
No	30	3.0	3.7	4.7	4.0	5.0
No	35	5.0	4.3	5.7	5.7	6.0
Moderate	20	3.5	3.3	4.7	4.7	4.0
Moderate	25	4.0	4.3	5.0	5.7	5.0
Moderate	30	4.5	4.7	5.0	5.0	7.0
Moderate	35	5.5	5.3	6.0	6.0	5.0
Light	25					
Moderate	25					
Heavy	25					
Severe	25					

Looking at the average Cooper-Harper ratings the following observations can be made. The first part shows an increasing rating with both the crosswind strength and the degradation of the runway condition. The addition of moderate turbulence in the second part clearly shows an increase of all ratings. The third

part also shows a clear increase of the ratings with the increase of the turbulence strength. The effect of turbulence or gusts should therefore be a factor in determining the crosswind limits.

Looking at the Cooper-Harper rating scale an acceptable workload or effort for the pilot to perform the required task corresponds with a rating of 3 “Minimal pilot compensation required for desired performance” or 4 “Desired performance requires moderate pilot compensation”. A rating of 5 “Adequate performance requires considerable pilot compensation” or higher is considered to be not acceptable for normal operations. To ensure safe execution of a landing in cross wind conditions there should be no need for the pilot to perform considerable compensation or at least this should not be expected.

Taking a rating of 4 as the maximum acceptable rating, the crosswind limits shown in Table 2-9 can be derived from the average Cooper-Harper ratings.

It should be noted that with only three pilots participating in the experiment firm conclusions cannot be drawn but the results do indicate the general trend.

**Table 2-9: Crosswind limits based on average Cooper-Harper ratings from the experiment (including moderate turbulence)**

Runway Condition	Crosswind Limit
Dry	25kts
Wet	20kts
Contaminated	5kts
Icy	5kts

Table 2-10 shows the guidance on crosswind limits given in the Aircraft Operating Manual of the Fokker 100. Table 2-11 indicates how the friction coefficients given in this table for the various braking action reports (GOOD/MEDIUM/POOR) correspond to the runway conditions used in this study. Comparing the crosswind limits from the aircraft operating manual to the values derived from the Cooper-Harper ratings shows that these numbers compare very well. In this sense it seems the results from the simulator experiment can be used to derive valid crosswind limits.

**Table 2-10: Maximum wind components (incl. gusts) for manual landings (runway width 45m or more)**

Braking Action	Friction Coefficient	Crosswind Limit
GOOD	$\geq 0.40$	30kts
MEDIUM	0.30 – 0.35	15kts
POOR	$\leq 0.25$	5kts

**Table 2-11: Correlation of runway condition to braking action for the speed range encountered in this study (below 120kts)**

Runway Condition	Friction Coefficient	Braking Action
Dry	0.67 – 0.86	GOOD
Wet	0.33 – 0.84	MEDIUM - GOOD
Contaminated	0.10 – 0.82	POOR - GOOD
Icy (Dry)	0.20	POOR
Icy (Melting)	0.06 – 0.14	POOR

#### 2.3.4. Analysis of Data Recordings

Besides the Cooper-Harper ratings from the pilots, all flight parameters are recorded for analysis. These are the objective data from the experiments. These data show how accurate the pilots were able to control the aircraft under all the different conditions. The objective of all the scenarios is to land the aircraft as close as possible to the centreline and keep the deviation from the centreline during the landing roll as small as possible. To see how well this objective has been achieved the results are presented in centreline deviation plots.

##### Baseline Scenario

In the baseline scenarios different crosswind strengths are assessed in the absence of turbulence. Also four different runway conditions are used in this baseline; dry, wet, contaminated and icy (dry ice). In Figure 2-8 these four runway conditions are presented in separate centreline deviation plots. The blue part represents the airborne part or the final approach of the flight. The green part represents the landing roll all the way to a complete stop of the aircraft.

First of all it can clearly be noted that the landing roll becomes longer with the degradation of the runway condition.

Another observation is that the deviations from the centreline are the largest for the contaminated runway. Looking at the maximum friction coefficient curves in Figure 2-5 this is no surprise. At higher speeds the friction coefficient for a contaminated runway is even lower than that of an icy runway. Just after touchdown this reduces the controllability significantly and it takes longer to correct the deviations from the centreline.

In general for all the baseline scenarios it can be stated that the deviations from the centreline stay well within the allowable runway limits. With crosswinds up to 35kts and even on icy runways this simulation model can be controlled to stay within the required runway limits. From the remarks of the pilots and looking at the Cooper-Harper ratings it should also be noted that in the extreme cases the pilots sometimes need to use maximum rudder and aileron control inputs to keep the aircraft under control.

This is certainly undesirable and cannot be classified as safe operation and is therefore outside of the capabilities of the aircraft and indicates the limit to which the aircraft can be operated.

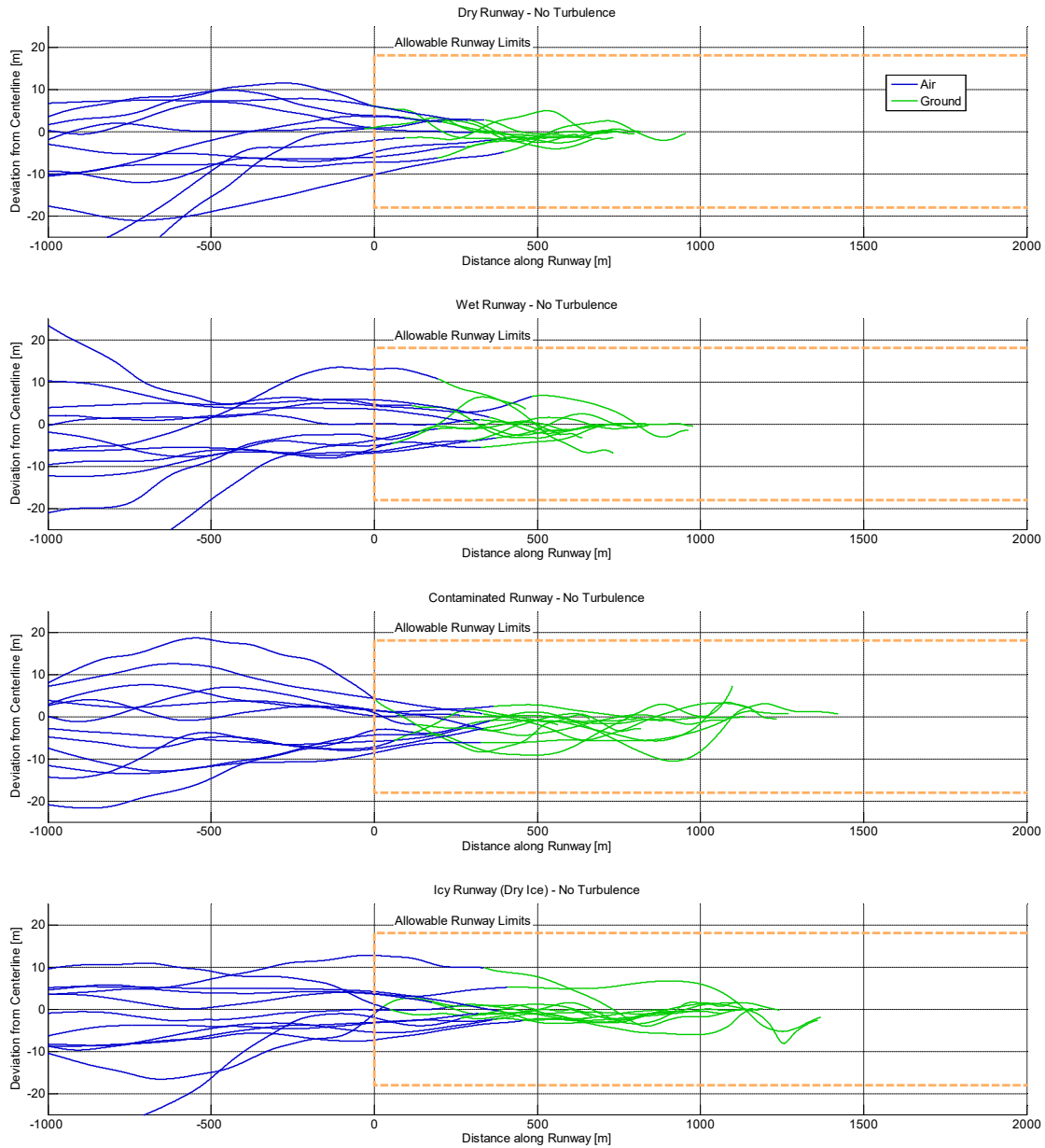


Figure 2-8: Final Approach and Landing Roll - No Turbulence - 4 Runway Conditions - Crosswinds between 20 and 35kts

### **Adding Moderate Turbulence**

The second part of the simulator experiments is basically a rerun of the first part but with the introduction of moderate Dryden turbulence. Comparing the results from the first and second part the effect of turbulence can be assessed. The results of the second part are presented in Figure 2-10. Comparing these results to those of the first part without turbulence shows mainly differences in the airborne or final approach part. This results in touchdowns with a larger deviation from the centreline. The deviations from the centreline seem to be the largest on the icy runway in this case. But looking in more detail these larger overall deviations are a result of the larger deviation at the initial touchdown point and the crab angle. The deviations and the required effort to correct these seem to be about the same on contaminated and icy runways.

### **Rudder Activity**

The previous section showed that the simulated Fokker 100 can still be controlled during approach and landing roll on an icy runway at a crosswind of up to 35kts. This is also valid with turbulence up to moderate strength. This is a little bit surprising because during flight tests with the Fokker 100 it was demonstrated that 35kts crosswind on a dry runway was on the edge of controllability. Crosswind tests are generally not performed on slippery or icy runways so there is no proof of match data for these conditions. It is therefore hard to say if the simulation models used in this study represent the icy runway conditions with sufficient realism.

To look at the amount of rudder required during approach and landing the recorded rudder inputs of the simulator sessions are averaged and splined. The results are presented in Figure 2-9. This figure shows plots for the different scenarios and both with and without moderate turbulence. The shapes of these plots do not differ much from each other. The only noticeable difference in these plots is between with and without turbulence in the first 40 seconds. This is the airborne phase of the recording. With turbulence it seems necessary to correct more with rudder in the approach phase. For the landing roll phase there seems to be no significant difference in the amount of rudder input required.

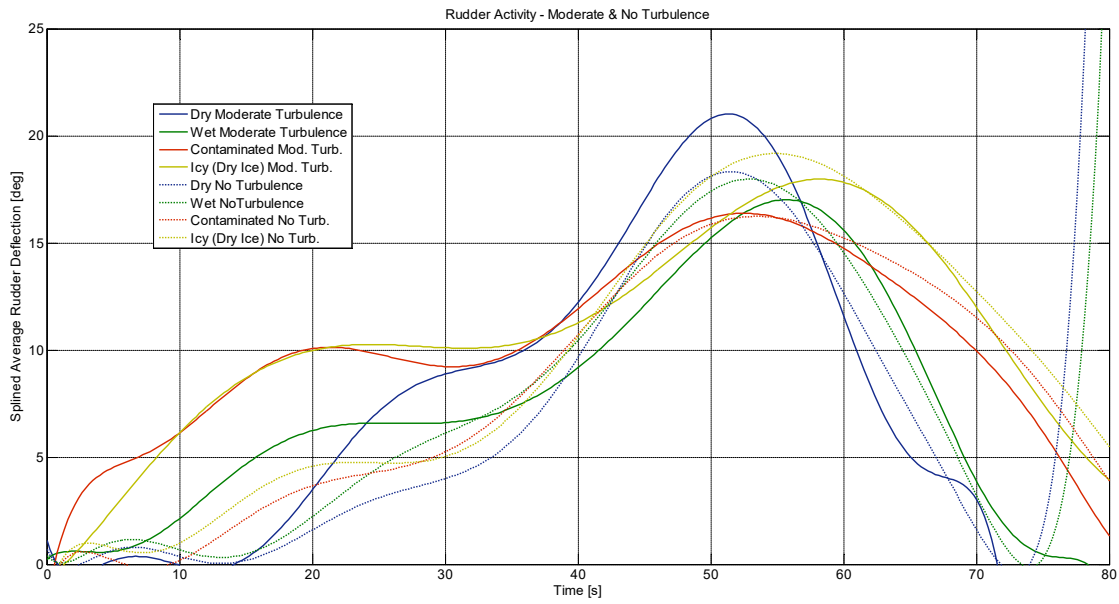
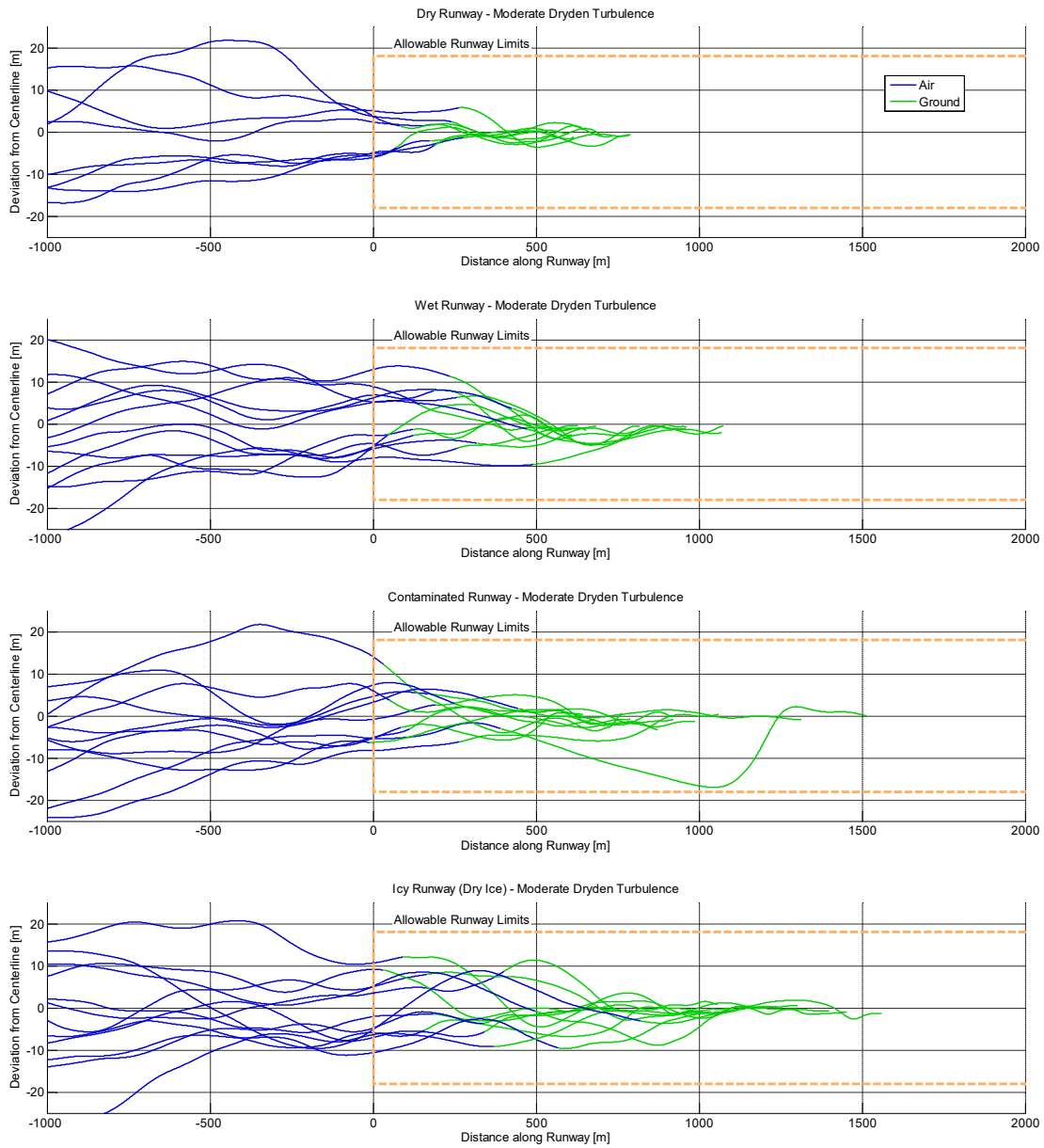


Figure 2-9: Rudder Activity during Approach and Landing Roll with Moderate and No Turbulence



**Figure 2-10: Final Approach and Landing Roll - Moderate Turbulence - 4 Runway Conditions - Crosswinds between 20 and 35kts**

## **Turbulence Levels**

In the third part of the simulator experiment the focus is on the influence of the level of turbulence. The scenarios for this part of the experiment use a fixed crosswind of 25kts and four different runway conditions (wet, contaminated, icy (dry ice) and melting ice). Four turbulence levels are compared (light, moderate, heavy and severe).

The results are presented in four runway centreline deviation plots, one for each turbulence level in Figure 2-11. Again it can be observed that a higher turbulence level results in larger deviations in the final approach up to the landing. The pilot has to work harder to arrive within the landing zone limits at the runway. This also leads to a less stabilised and not completely aligned landing. If the landing is not aligned or not fully de-crabbed this requires more corrections during the landing roll to return to the centreline.

Looking at the landing roll part it can be observed that at the higher turbulence levels the crab angles are larger and the resulting corrections result in larger deviations from the centre line. On a contaminated runway or a runway with melting ice the deviations from the centreline are clearly the largest. In one case on a contaminated runway the aircraft even left the runway.

The influence of the turbulence seems to have little effect on the landing roll itself. The largest effect is on the approach and the resulting centreline deviation and crab angle at touchdown.

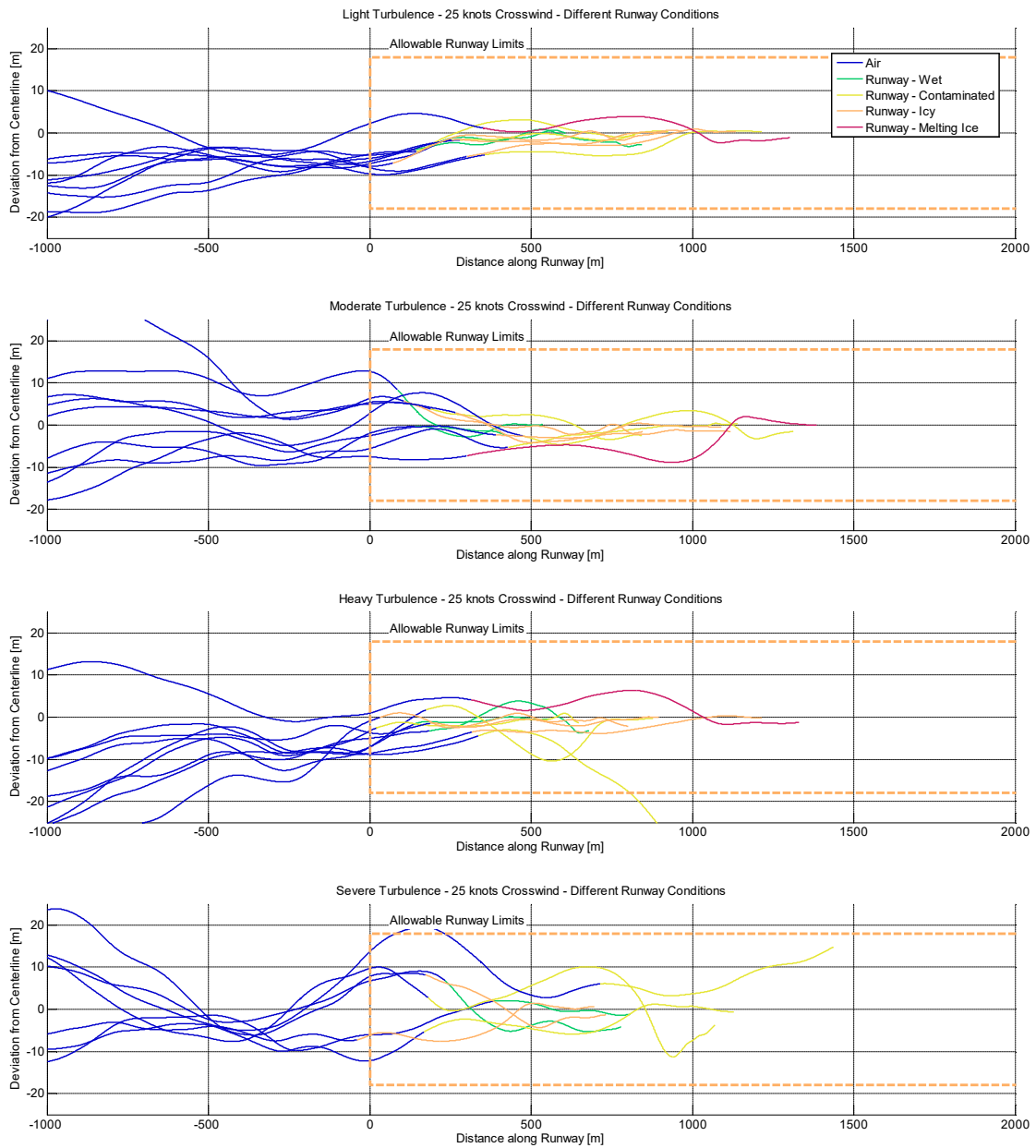


**Figure 2-11: Final Approach and Landing Roll - 25kts Crosswind - 4 Turbulence Levels - Various Runway Conditions**

## 2.4. Fast-Time Simulations

The fast-time simulations have been executed in the MATLAB-Simulink simulation environment using the offline version of the Fokker 100 aircraft model (which is identical to the Fokker 100 simulator model) extended with a pilot model, as described in section 2.2. This section describes the setup of the fast-time simulations and discusses the results.

### 2.4.1. Baseline Scenario

For the fast-time simulations a baseline scenario has been defined. Variations in crosswind and runway condition as specified in the test matrix (see section 2.4.2) and variations in the modelling configuration (as specified in section 2.4.3) have been applied to this baseline scenario.

The baseline scenario starts at an altitude of 200ft AGL. The aircraft is in landing configuration with flaps 42, gear down and speed brakes extended as recommended in the AOM for landing on contaminated/slippery runways. The aircraft is trimmed at a final approach speed of 135kts (which includes a wind correction factor of 10kts). The wind speed is 40kts (at 10m).

In crosswind conditions a crabbed approach is performed, i.e. the aircraft is headed into the wind with wings level. A full decrab is initiated at 100ft by applying into-wind aileron and opposite rudder. The flare is initiated at 30-50ft depending on the wind conditions. The flare altitude increases from 30ft for headwind only to 50ft for crosswind only.

After touchdown, the thrust reversers are deployed at main gear weight on wheels detection and maximum braking is applied (at nose gear weight on wheels detection). When the runway condition is icy, full reverse is applied. In other conditions the standard idle reverse is used. The simulation is stopped when the ground speed is less than 5kts.

Table 2-12 gives an overview of the input parameters and (initial) conditions used in the baseline scenario.

**Table 2-12: Input parameters and (initial) conditions for the baseline scenario**

Parameter	Value	Remarks
Gross Weight	34,000kg	
CG	30, 0, -0.6	x (%mac), y (%span), z (%mac)
Flaps	42deg	full landing flaps
Gear	down	
Speed Brakes	extended	
$V_{REF}$	120kts	IAS
FAS	135kts	$V_{REF} + 5kts + WCF (10kts)$

Parameter	Value	Remarks
GPA	3deg	
Initial Altitude	200ft AGL	
Decrab Altitude	100ft AGL	
Decrab Angle	full	
Flare Altitude	50 / 30ft AGL	50ft in pure crosswind, 30ft in pure headwind
Braking	full	
Reversers	idle/full	full reverse when runway condition is icy
Wind Speed	40kts	at 10m
Wind Direction	variable	see test matrix
Atmospheric Conditions	ISA	
Field Elevation	sea level	
Runway Condition	variable	see test matrix
Turbulence	none	

#### 2.4.2. Test Matrix

Using the baseline scenario, the crosswind and runway conditions are varied in a test matrix to assess their effect on the directional control of the aircraft on the runway and to determine appropriate crosswind limits for each runway condition. While the wind speed in the simulations is kept constant at 40kts (at 10m), the wind direction is varied from 0 to 90 degrees to expose the aircraft to the desired range of crosswind components (0 - 40kts). Using steps of 2.5kts a total number of 17 crosswind conditions have been simulated. In addition, five different runway conditions have been investigated, leading to a total number of 85 simulation runs. Table 2-13 summarizes the test matrix.

**Table 2-13: Test matrix**

Parameter	Values
Crosswind Component	0 - 40kts (2.5kts steps)
Runway Condition	dry, wet, contaminated, icy (dry), icy (melting)

### 2.4.3. Alternative Modelling Configurations

In the baseline modelling configuration the standard Fokker 100 landing gear model is used and the simulations have been performed at 100Hz. Furthermore, the baseline configuration does not include turbulence. To investigate the effect of the modelling configuration on the determination of crosswind limits, the test matrix described in the previous section has also been applied to several alternative configurations, i.e.:

- Smaller simulation time step (600Hz) to more accurately simulate the high frequency dynamics of (particularly) the landing gear
- Including a different, more basic, landing gear model
- Including turbulence using different models (Dryden, NLR) and intensity levels (light, severe)

Table 2-14 lists the configurations that have been investigated.

**Table 2-14: Modelling configurations**

Parameter	Baseline Configuration	Alternative Configuration(s)
Simulation Time Step	0.01s (100Hz)	0.0017s (600Hz)
Landing Gear Model	Fokker 100	Generic
Turbulence Model	none	Dryden, NLR
Turbulence Level	none	Light, Severe

### 2.4.4. Model Checkout

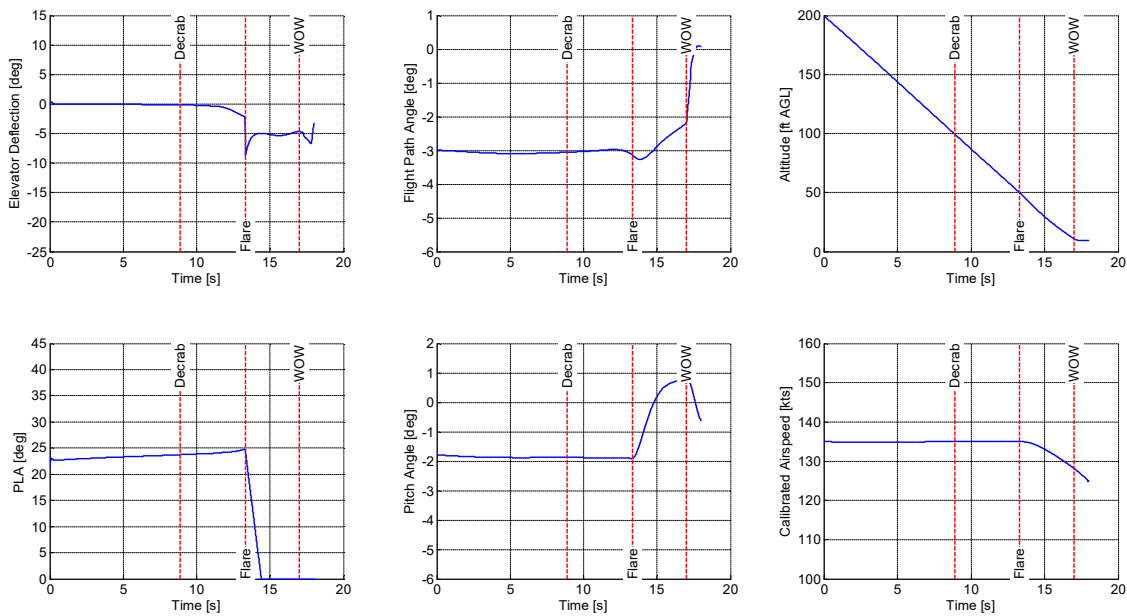
To ensure that the model used in this study is fit for the purpose the data of several simulation runs have been evaluated by investigating the time traces of relevant parameters and verifying that the behaviour of the aircraft is as expected. The main concern is the whether the pilot model is able to control the aircraft in the extreme conditions that are simulated (such as a combination of strong crosswind and severe turbulence).

Figure 2-12 through Figure 2-14 show time traces from a simulation run in the baseline scenario with a crosswind of 40kts and a dry runway. In the absence of turbulence and with a trimmed aircraft the pilot model has no difficulty in performing the landing. It is noticeable though that a full decrab cannot be accomplished due to insufficient rudder authority, which is not surprising as a 40kts crosswind is outside the limits for a F100. However, this has no effect on the directional control. The aircraft remains within a few meters of the centreline.

Figure 2-15 through Figure 2-17 show the performance in a 20kts crosswind with severe Dryden turbulence and on an icy (dry ice) runway. It can be seen that it takes the pilot model a significant effort to control the aircraft. In the airborne phase this is most apparent by looking at the elevator and rudder

deflections. Maximum control surface deflections are applied repeatedly indicating that the aircraft is performance limited in these conditions. In the ground run it can be seen that the pilot model is barely able to keep the aircraft on the runway, with a maximum deviation of almost 15m from the centreline. However, this is not surprising as the 20kts crosswind is well above the advised crosswind limit on this runway condition.

Overall, the pilot model performance seems adequate and the model thereby fits the purpose.



**Figure 2-12: Longitudinal control in the baseline scenario (40kts crosswind, dry runway)**

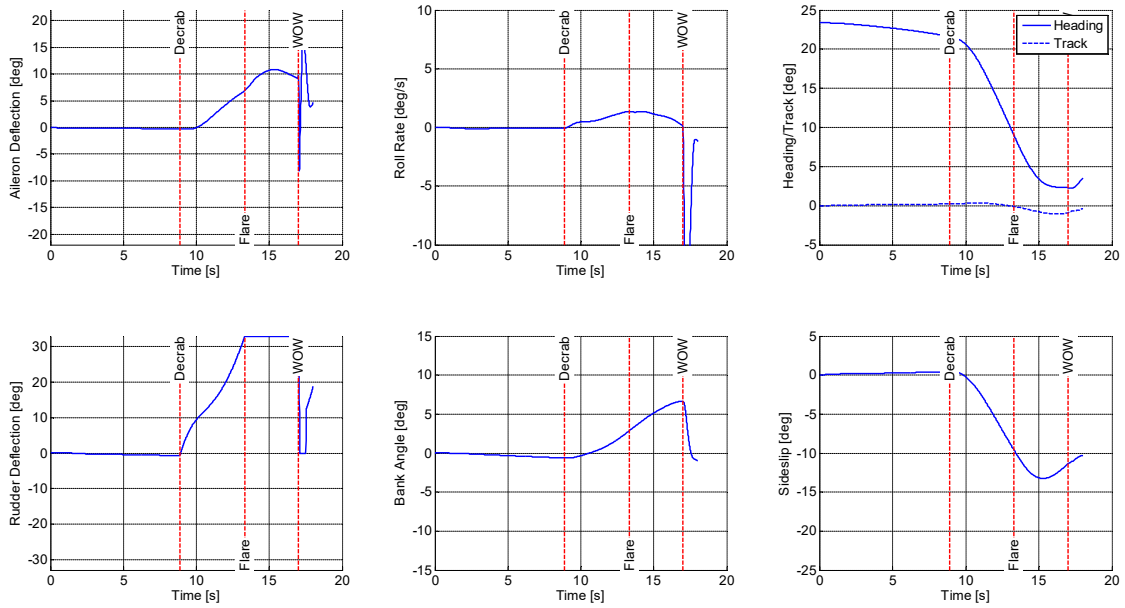


Figure 2-13: Lateral control in the baseline scenario (40kts crosswind, dry runway)

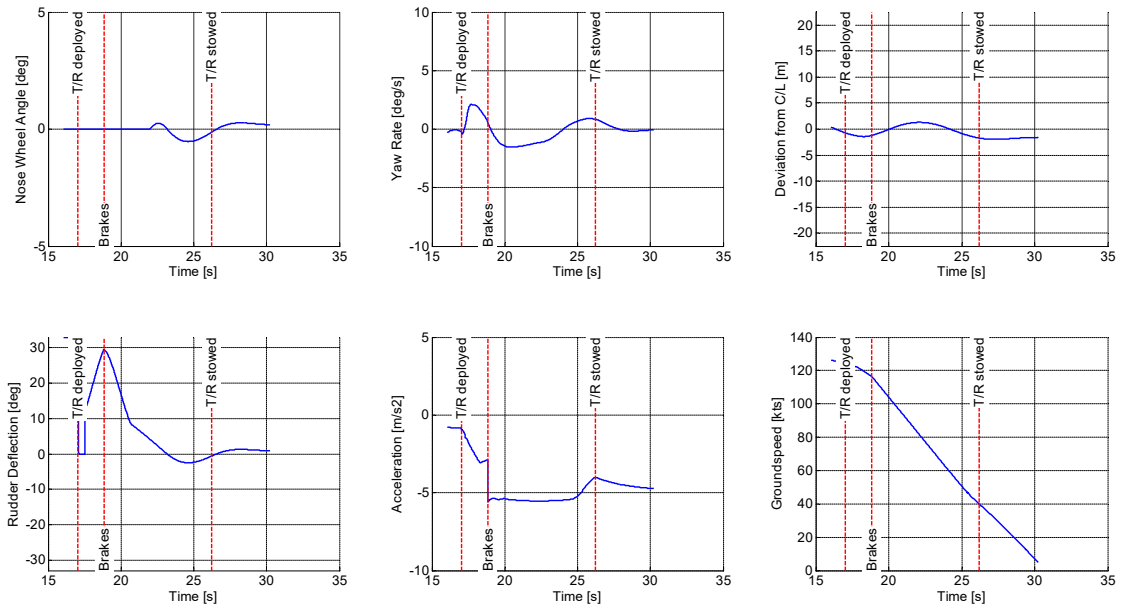


Figure 2-14: Directional control in the baseline scenario (40kts crosswind, dry runway)

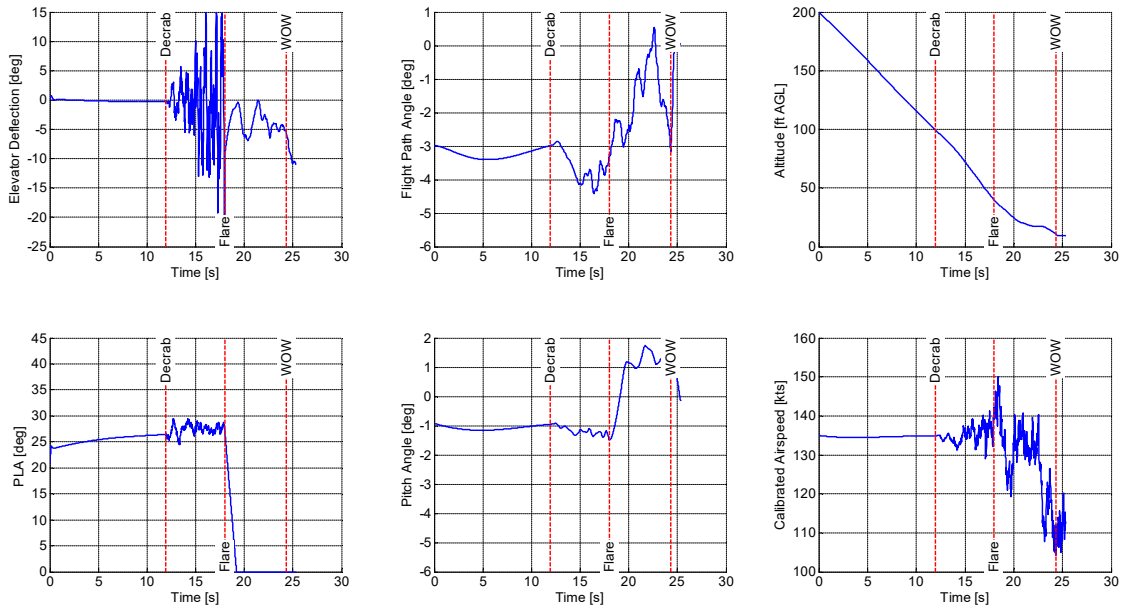


Figure 2-15: Longitudinal control in severe Dryden turbulence (20kts crosswind, icy (dry ice) runway)

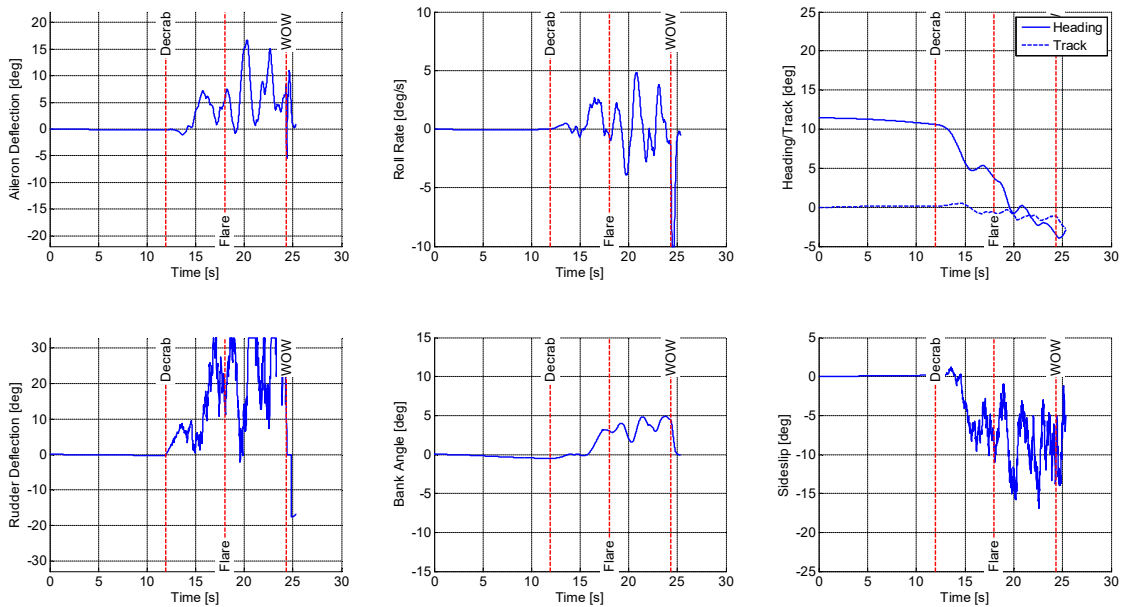
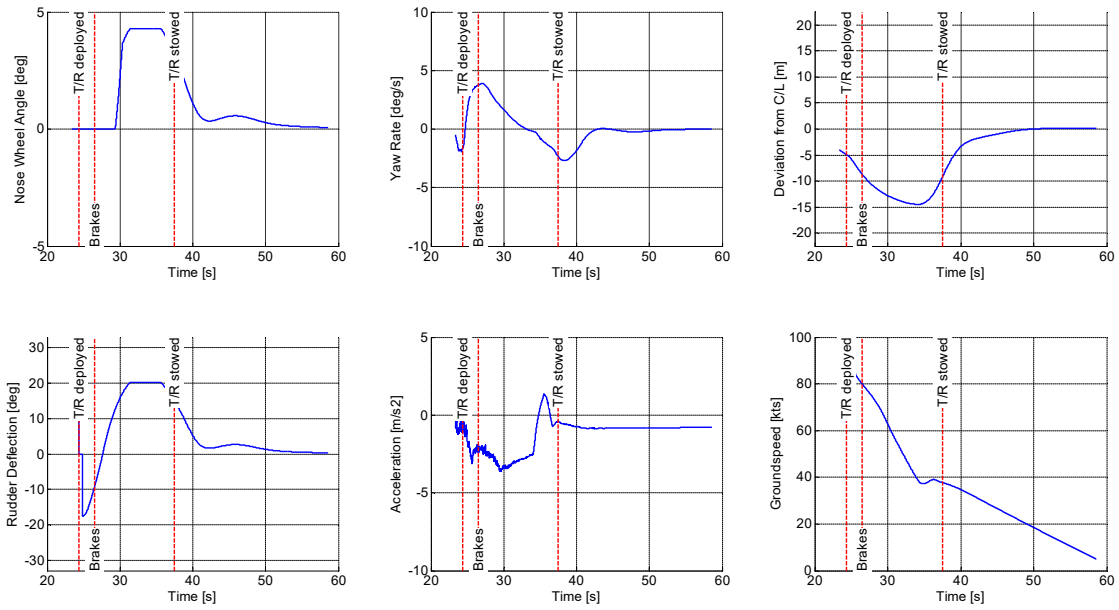


Figure 2-16: Lateral control in severe Dryden turbulence (20kts crosswind, icy (dry ice) runway)



**Figure 2-17: Directional control in severe Dryden turbulence (20kts crosswind, icy (dry ice) runway)**

### 2.4.5. Comparison between Simulator and Fast-Time Results

Certain scenarios are both used for the fast-time simulations and the simulator experiments. The results of three of these scenarios are compared in this section. These three scenarios are:

- 25kts crosswind - dry runway - no turbulence (Figure 2-18)
- 25kts crosswind - contaminated runway - no turbulence (Figure 2-19)
- 25kts crosswind - contaminated runway - severe Dryden turbulence (Figure 2-20)

In general the trend and the average magnitude of the control inputs of both the real pilot and the simulated pilot (pilot model) show significant resemblance. The simulated pilot tends to control the aircraft with smoother control commands where the real pilot uses more smaller corrections to arrive basically at the same aircraft path control. Looking at the centreline tracking the real pilot in the end does a slightly better job. The experience and skills of the real pilot gives him a definite advantage. This is hard to match with a model without it getting very complex and sophisticated. But it can be concluded that the pilot model that is constructed for this study does a pretty good job and performs not much different from a real pilot.

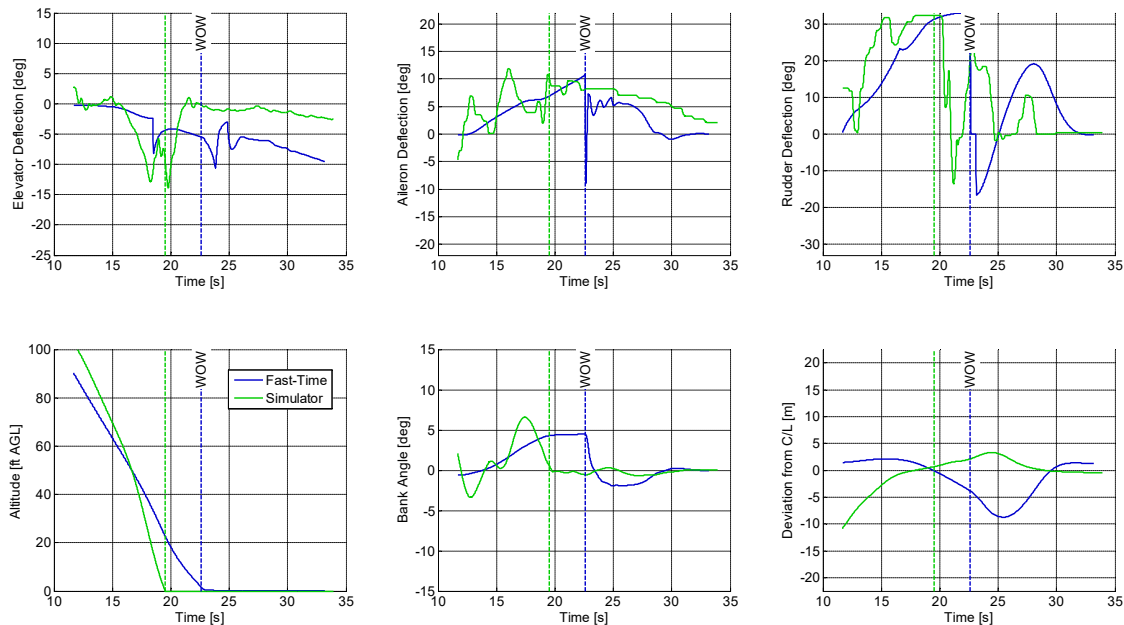


**Figure 2-18: Comparison between Simulator and Fast-Time - 25kts Crosswind - Dry Runway - No Turbulence**

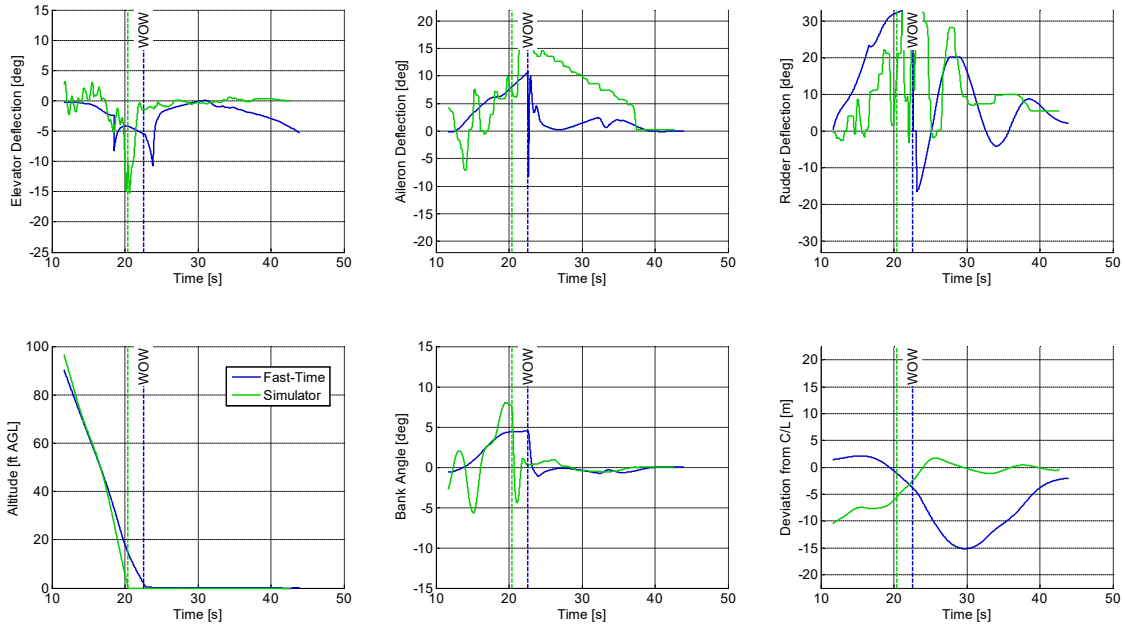


Figure 2-19: Comparison between Simulator and Fast-Time - 25kts Crosswind - Contaminated Runway - No Turbulence

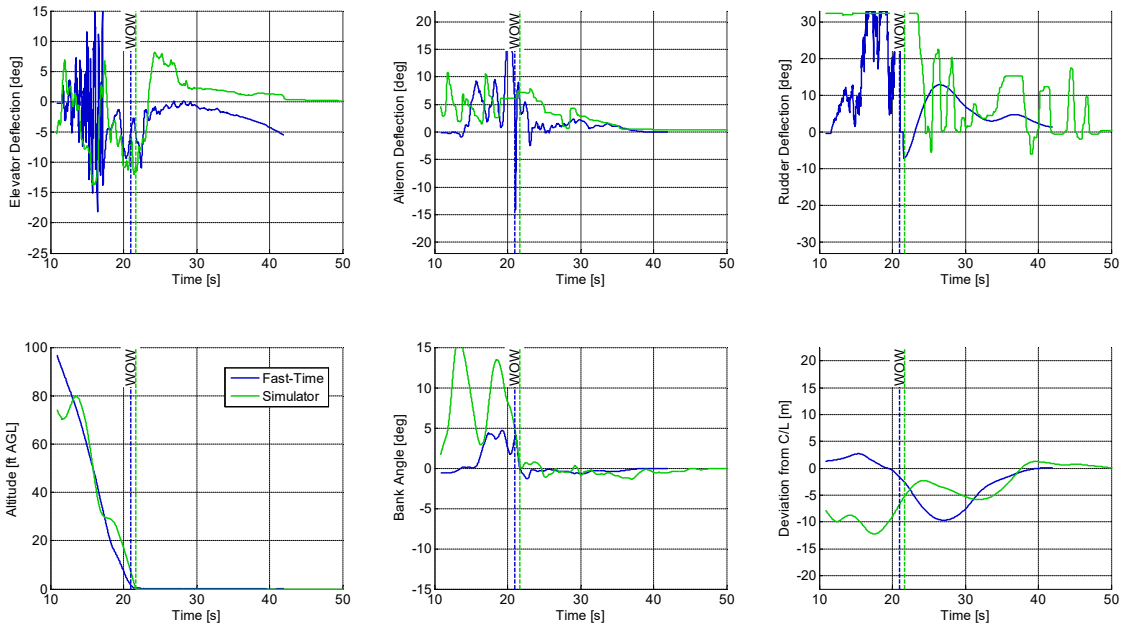
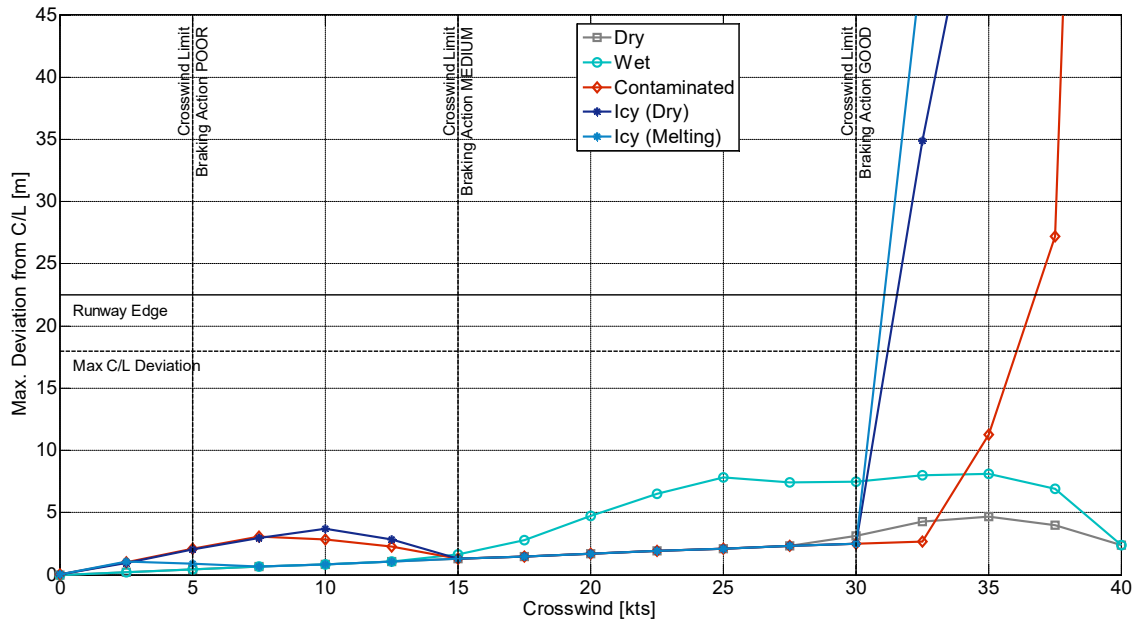


Figure 2-20: Comparison between Simulator and Fast-Time - 25kts Crosswind - Contaminated Runway - Severe Dryden Turbulence

### 2.4.6. Crosswind Limits

Figure 2-21 shows the maximum deviation from the centreline during the ground run for the various crosswind and runway conditions that have been simulated in the baseline scenario. Each marker corresponds to a specific simulation run. Also indicated in this figure is the edge of the runway (with a standard width of 45m) and the maximum deviation of 18m as used in the certification of automatic landing systems<sup>1</sup>. It can be seen that for dry and wet runway conditions the pilot model is able to keep the aircraft on the runway, even in 40kts crosswind conditions. Apparently, in these conditions the friction is sufficient to generate the side forces required to counter the aerodynamic side force produced by the crosswind. When the runway is contaminated or icy however, a sharp increase in the centreline deviation can be observed starting at a crosswind of 30 to 35kts. This suggests that at this point the friction becomes insufficient and directional control is lost. The pilot control model, in its effort to turn the aircraft towards the centreline, further increases the nose wheel steering angle and thereby the slip angle, which only deteriorates the situation. In real-life the proper action would be to reduce the slip angle to regain traction of the nose wheel. However, this logic has not been incorporated in the basic directional control model used in this study.



**Figure 2-21: Maximum deviation from the centreline for various crosswind and runway conditions (baseline scenario and modelling configuration)**

<sup>1</sup> EASA CS-AWO 131 prescribes that a lateral touchdown with the outboard landing gear more than 21m from the centreline shall be improbable. Accounting for a distance of 3m between the outboard landing gear and the CG of the aircraft, this leads to a maximum deviation of 18m.

Figure 2-21 also shows that the maximum deviation of 18m is exceeded at relatively high crosswinds (30-35kts on contaminated/icy runways and >40kts on dry/wet runways). These crosswind values are significantly higher than the crosswind limits given in the Operations Manual of the operator (see Table 2-10). This shows that the crosswind that actually exceeds the capacity of the aircraft to counter the side forces generated by the crosswind in the landing roll is not the primary factor in determining the crosswind limits. The main factor is the acceptability of the controllability demand on the pilot and whether sufficient control authority is available.

#### 2.4.7. Effect of Variations in Modelling Configurations

As described in section 2.4.3, the fast-time simulations have also been conducted using alternative modelling configurations to investigate the impact of these variations on the determination of crosswind limits.

Figure 2-22 shows the maximum deviation from the centreline based on simulations performed using the generic, less sophisticated, landing gear model instead of the standard Fokker 100 model. It can be seen that this has a significant impact on the results. For contaminated and icy runway conditions the maximum deviation from the centreline observed in the simulations is much less suggesting that sophistication of this simplified model is insufficient to accurately model the dynamics in the ground roll.

Figure 2-23 through Figure 2-26 show the results of the simulations that include turbulence (light/severe NLR and Dryden turbulence respectively). The figures indicate that the impact of adding turbulence to the simulation is minor and that the type of turbulence has no significant effect on the results. The changes compared to the baseline (no turbulence) modelling configuration are small. This may seem surprising considering the clear increase in the Cooper-Harper ratings given by the test pilots in the simulator experiment with increasing turbulence. However, these ratings account for the increase in workload and control authority needed to control the aircraft, especially in the airborne phase. The pilot model however does not care about the workload required. Furthermore, the analysis of the data recordings of the simulator sessions has shown that in moderate turbulence the test pilots were able to keep the aircraft within 10m of the centreline, even though this took more effort.

Finally, Figure 2-27 shows the results based on simulations performed at a higher simulation frequency (600Hz). The results are identical to the baseline modelling configuration (at a 100Hz frequency). This shows that either the high-frequency dynamics of the Fokker 100 landing gear model are accurately captured at 100Hz or that they do not play a role in determining the crosswind limits.

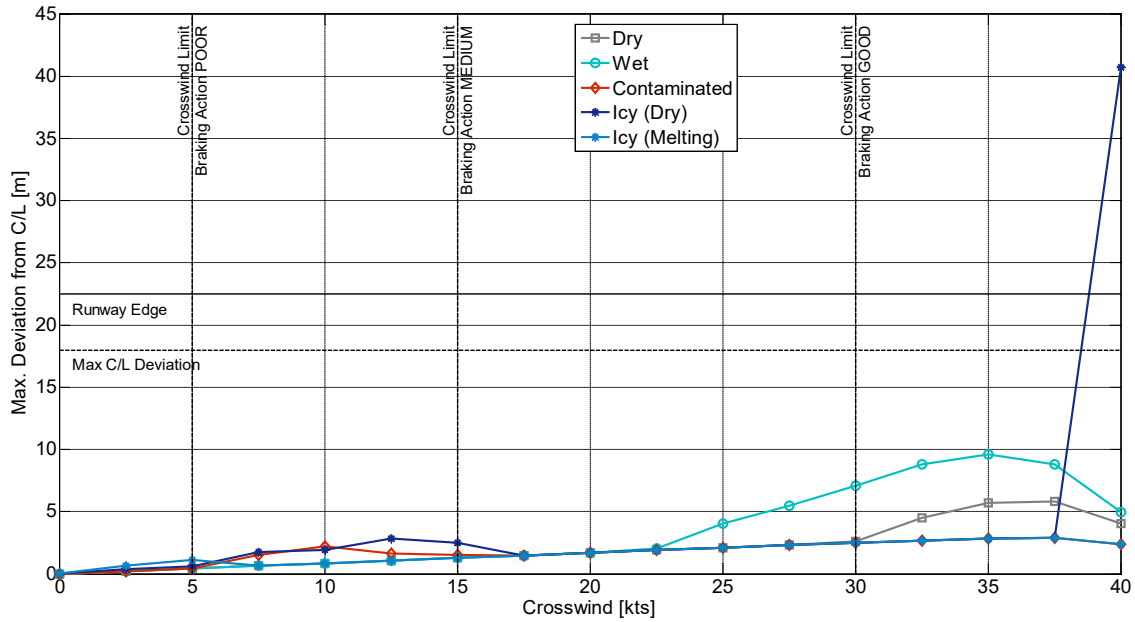


Figure 2-22: Maximum deviation from the centreline for various crosswind and runway conditions using the generic landing gear model

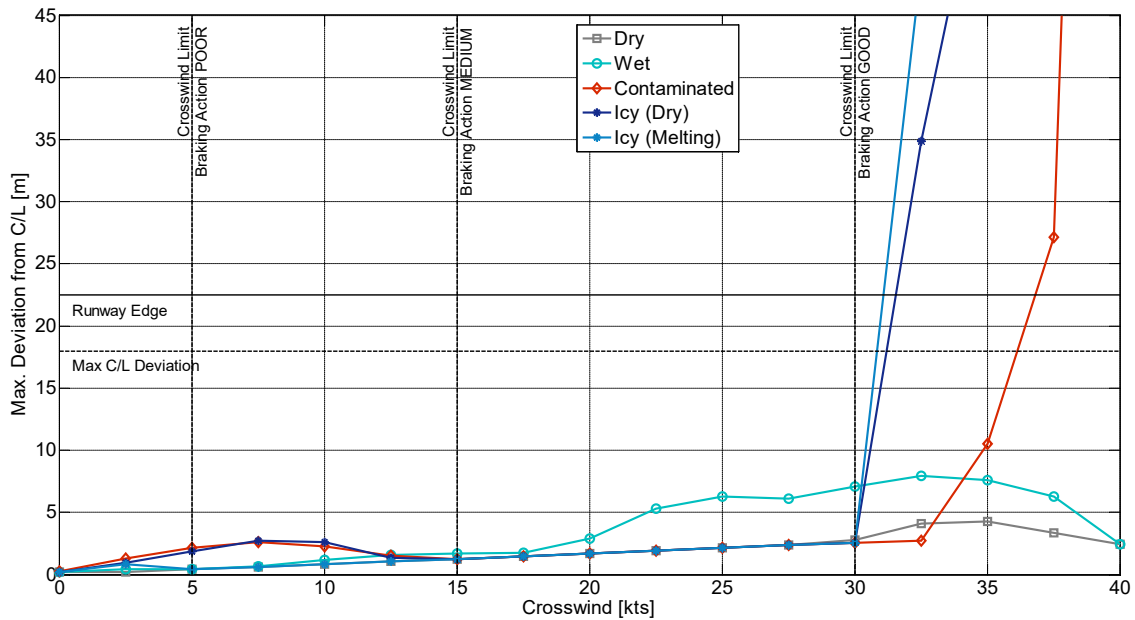


Figure 2-23: Maximum deviation from the centreline for various crosswind and runway conditions in light NLR turbulence

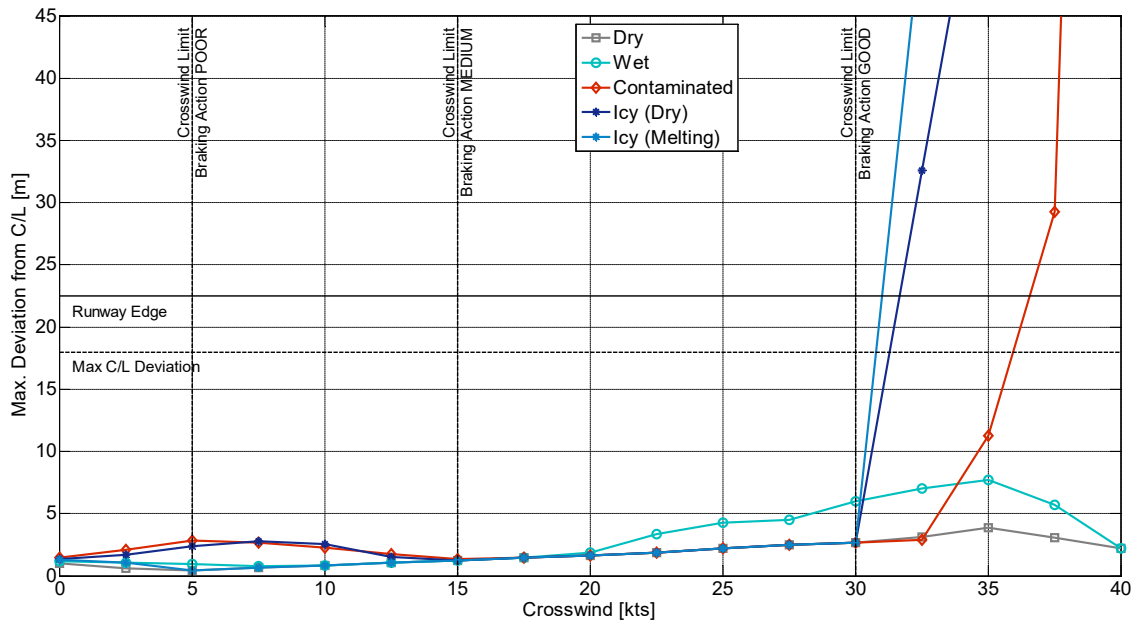


Figure 2-24: Maximum deviation from the centreline for various crosswind and runway conditions in severe NLR turbulence

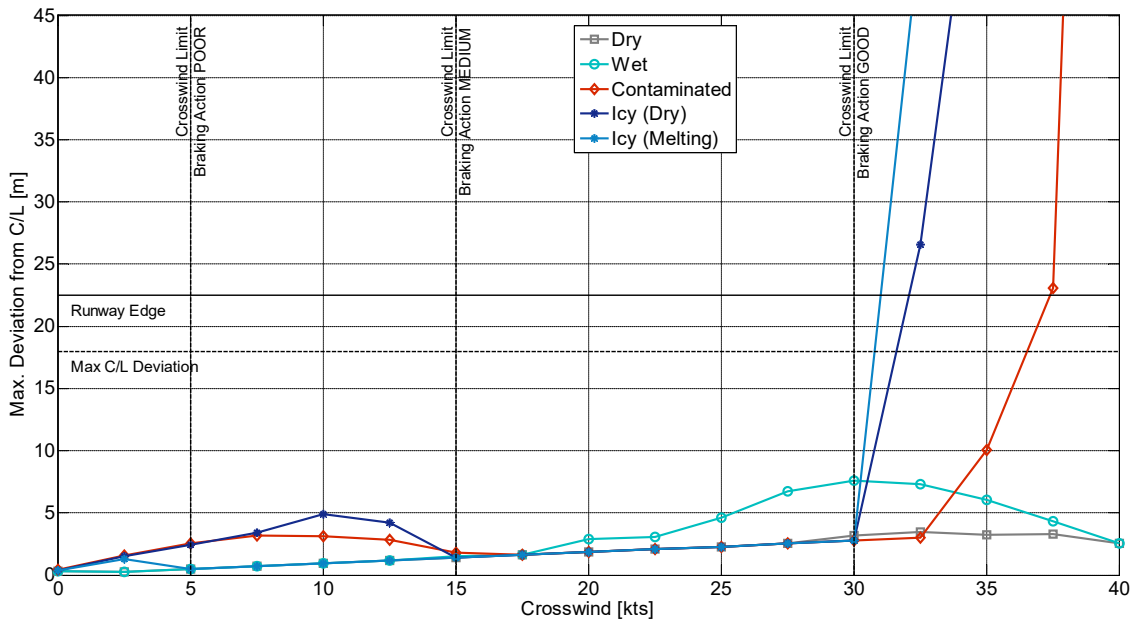
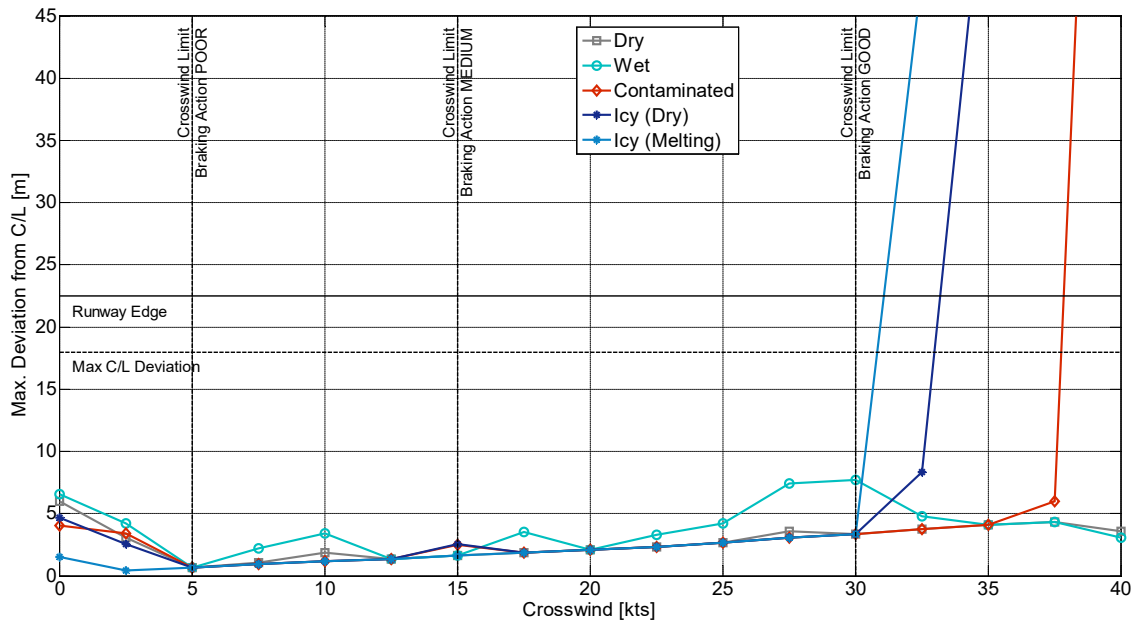
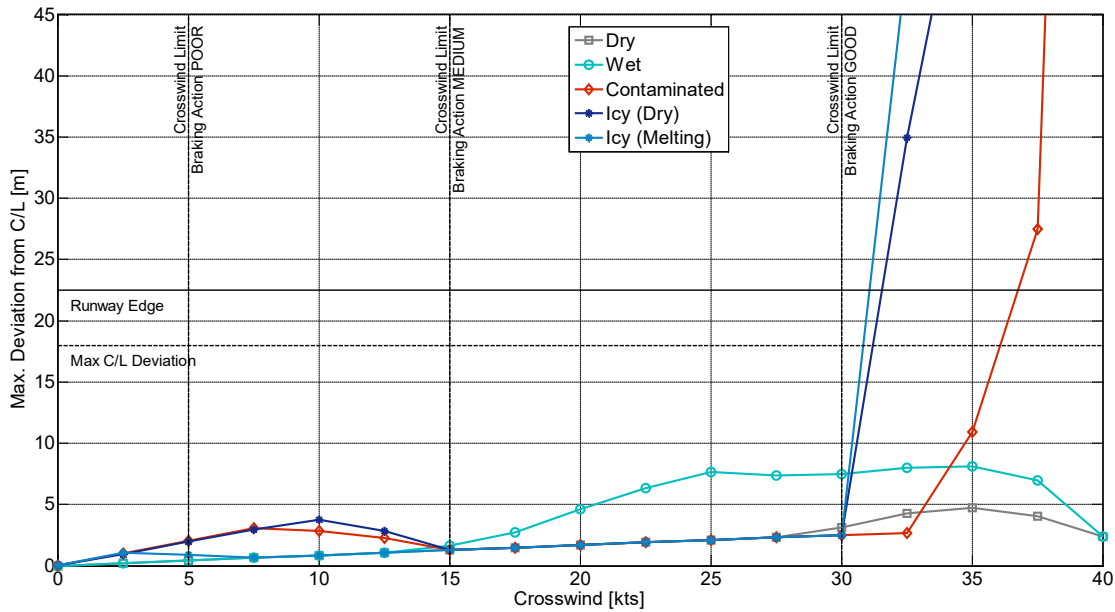


Figure 2-25: Maximum deviation from the centreline for various crosswind and runway conditions in light Dryden turbulence



**Figure 2-26: Maximum deviation from the centreline for various crosswind and runway conditions in severe Dryden turbulence**



**Figure 2-27: Maximum deviation from the centreline for various crosswind and runway conditions in the baseline scenario simulated at 600Hz**

## 2.5. Conclusions

The results from the simulator experiments and fast-time simulations show that there is a significant difference between the maximum crosswind that is considered acceptable by pilots in terms of controllability demands and the crosswind that actually exceeds the capacity of the aircraft to counter the side forces generated by the crosswind in the landing roll. The first leads to significantly lower crosswind limits and is the primary factor in the determination of these limits. Because the workload for pilots cannot be assessed in fast-time simulations, simulator experiments are essential.

While turbulence seems to have little effect on the crosswind at which the aircraft loses the ability to generate the required side forces to retain directional control in the ground roll, it does have a major impact on the control efforts required by the pilot, especially in the airborne phase. It is therefore essential that turbulence is included in simulator experiments aimed at determining crosswind limits.

The fast-time simulations show that the level of sophistication of the landing gear model has an impact on the assessment of crosswind limits. The landing gear model should at least account for the interaction between side and braking friction. Standard landing gear models like the Fokker 100 model account for these effects. Using even more sophisticated models that more accurately reflect the high frequency dynamics of the landing gear at touchdown and wheel spin-up may lead to more realistic ground reaction forces. But as the crosswind limits are mainly determined by the pilot workload in controlling the aircraft, the benefit of using such models is questionable. When a standard landing gear model is used, a basic update rate (100Hz) is sufficient.

Finally, it is noted that, due to a lack of test data, the accuracy of aerodynamic models in low speed and/or high sideslip conditions is questionable. This may have a significant impact on the fidelity of simulations to assess crosswind limits. This potential shortcoming could not be assessed in this study, but is further addressed in a separate activity within Task 3.1.4.

## 3 SIGNIFICANCE OF PROVIDING LOAD FACTORS INFORMATION

### 3.1. Introduction

The structure of this chapter is as follows:

- Section 2 describes the development of the simulation model.
- Section 3 describes the setup and results of the simulations.
- Section 4 gives the conclusions and recommendations.

### 3.2. Development of the model of forces and moments affecting the aircraft motion under conditions of strong crosswind and various types of runway contamination

Mathematic model of typical commercial airliner motion during takeoff and landing consists of the following interacted blocks.

- Ordinary well-known equations of spatial motion and corresponding kinematical relationships.
- Calculation of forces and moments generated by the engines operation.
- Engine dynamics.
- Dynamics of aerodynamic control surfaces actuators.
- Flight control system (FCS) algorithm.
- Calculation of aerodynamic forces and moments.
- Calculation of forces and moments generated by the contacts with RUNWAY surface.

In the context of this work only the last 2 block are of special interest — it is assumed that just their enhancement may significantly raise simulation accuracy from viewpoint of RUNWAY excursion problem and including veer off.

#### 3.2.1. Calculation of aerodynamic forces and moments

The main particularities of aerodynamic model under considered conditions are the following:

- Ground effect.
- Effect of extremely large sideslip angle — significantly more as compared to normal in-flight angles and with the angles typically investigated in wind tunnels.

There is used in described work some practically reasonable assumption that the ground speed magnitude is substantially more than magnitude of wind speed: ( $|V_k| \gg |W|$ ). This inequality is equivalent to condition where sideslip angle belongs to the most practically important region of  $\pm 90^\circ$ . So, air stream does not approach from backward semisphere of the aircraft. It may happen only for very low speeds that are of no interest in practice from viewpoint of veer off risk.

During ground run with large sideslip angles  $|\beta| > 25^\circ$ - $30^\circ$  aerodynamic characteristics significantly differ from characteristics at typical in-flight angles not more than  $15^\circ$ . The most important is effect of sideslip on directional stability and rudder effectiveness. Averaged wind tunnel characteristics of typical commercial airliner with takeoff flaps and undeflected control surfaces are presented on the next Figure 3-1, Figure 3-2, Figure 3-3:

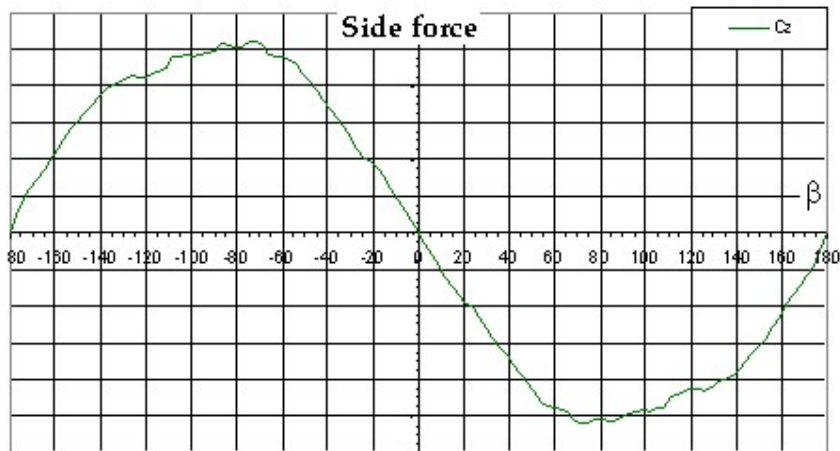


Figure 3-1: Circle diagram of side force versus sideslip angle dependency

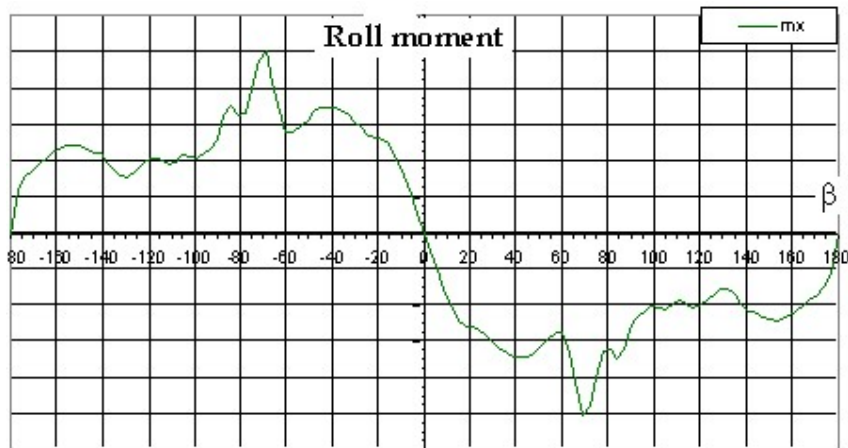
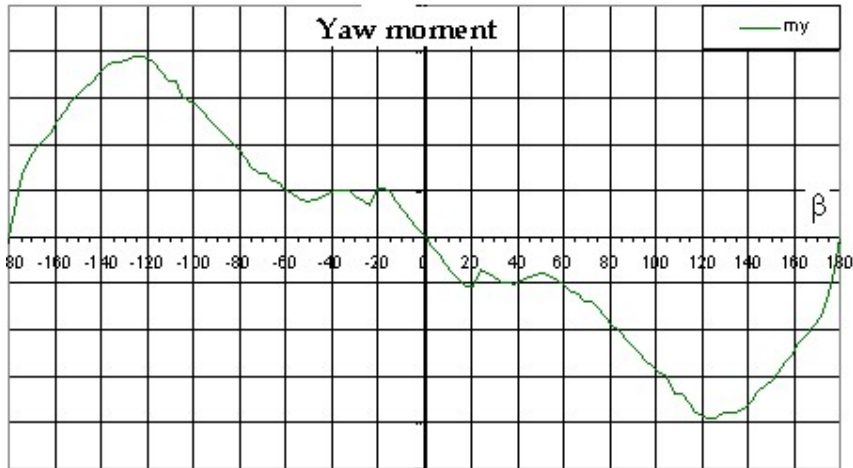
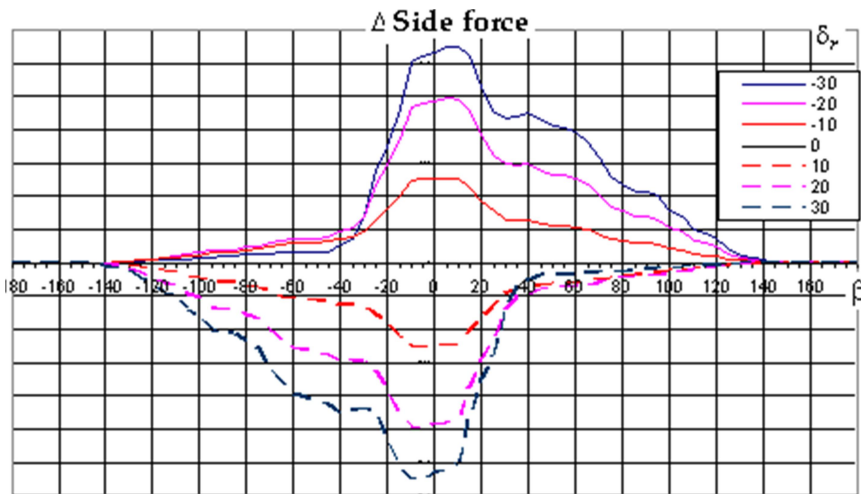


Figure 3-2: Circle diagram of roll moment versus sideslip angle dependency



**Figure 3-3: Circle diagram of yaw moment versus sideslip angle dependency**

Corresponding increments of aerodynamic coefficients characterizing effectiveness of rudder ( $\delta_r$ ) deflections are presented below in Figure 3-4, Figure 3-5, Figure 3-6:



**Figure 3-4: Circle diagram of rudder efficiency as to side force**

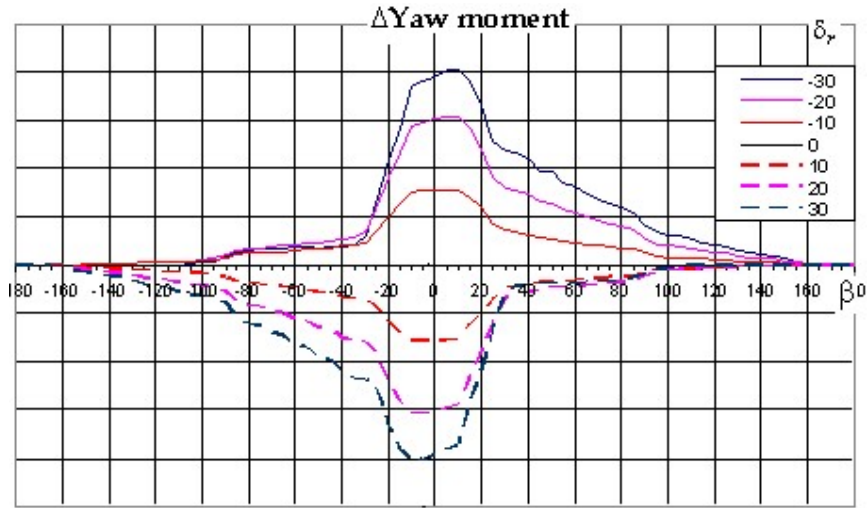


Figure 3-5: Circle diagram of rudder efficiency as to roll moment

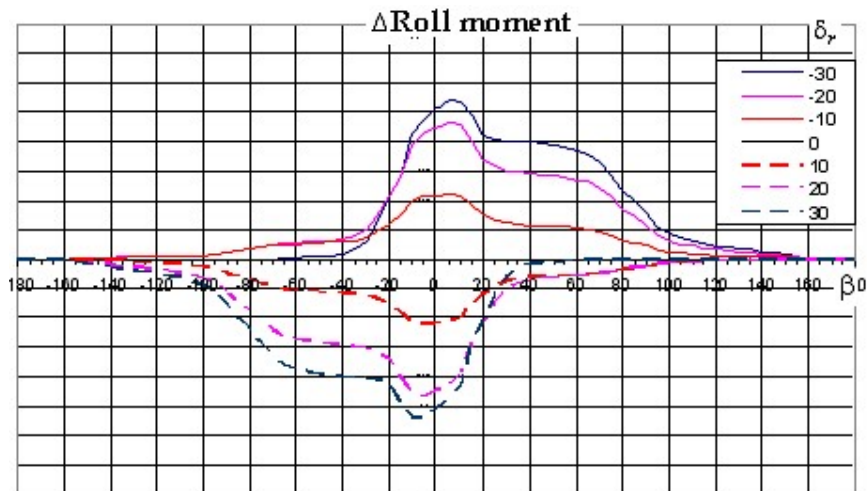


Figure 3-6: Circle diagram of rudder efficiency as to yaw moment

It may be seen that depicted dependences are very non-linear, and just such aerodynamic characteristics should be used for simulation of ground run.

### 3.2.2. Calculation of forces and moments generated by the contacts with runway surface

The report contains detailed description of the model of forces and moments of multi-wheel landing gear (LG) and RUNWAY surface interaction for typical commercial airliner. The main features of this model are described below.

It takes into account all the relevant characteristics of LG design and geometry, basic features of the pneumatics, shock absorbers parameters. The model of forces and moments affecting the aircraft from

RUNWAY surface is quasi-static — high-frequency motions of the wheels are neglected, movable components of LG are assumed to be weightless (as compared with aircraft weight), all the elastic deformations of aircraft and its LG are also weightless.

There are used adequate diagrams of shock absorbers and pneumatics looking as follows (Figure 3-7, Figure 3-8):

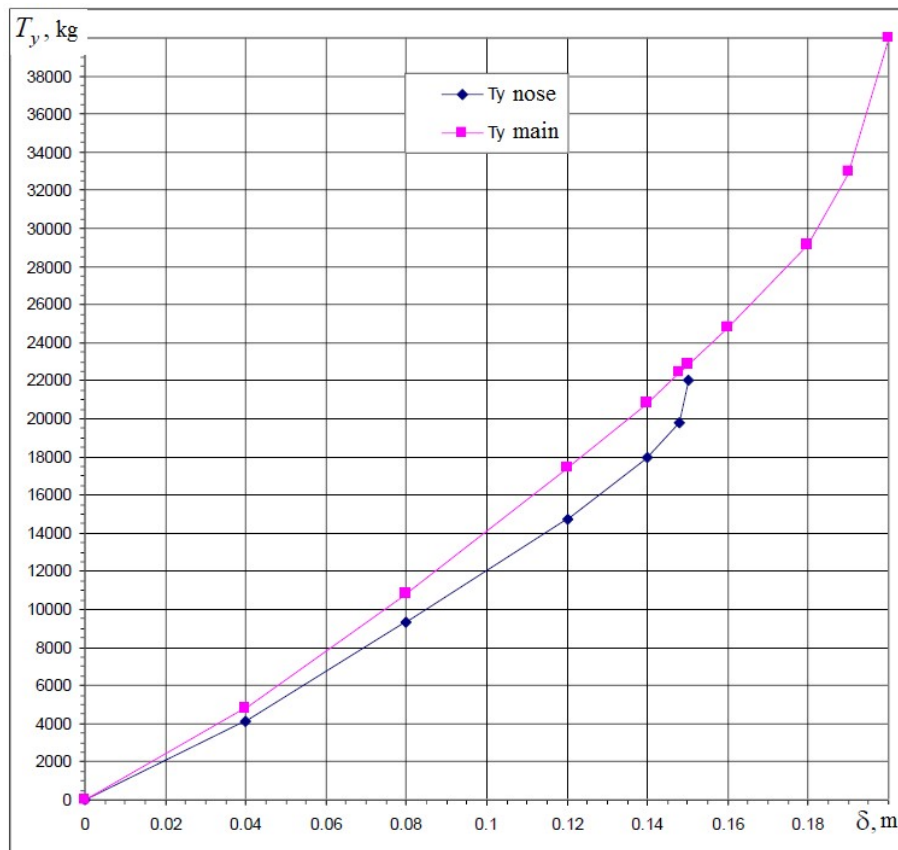


**Figure 3-7: Diagram of pneumatics**

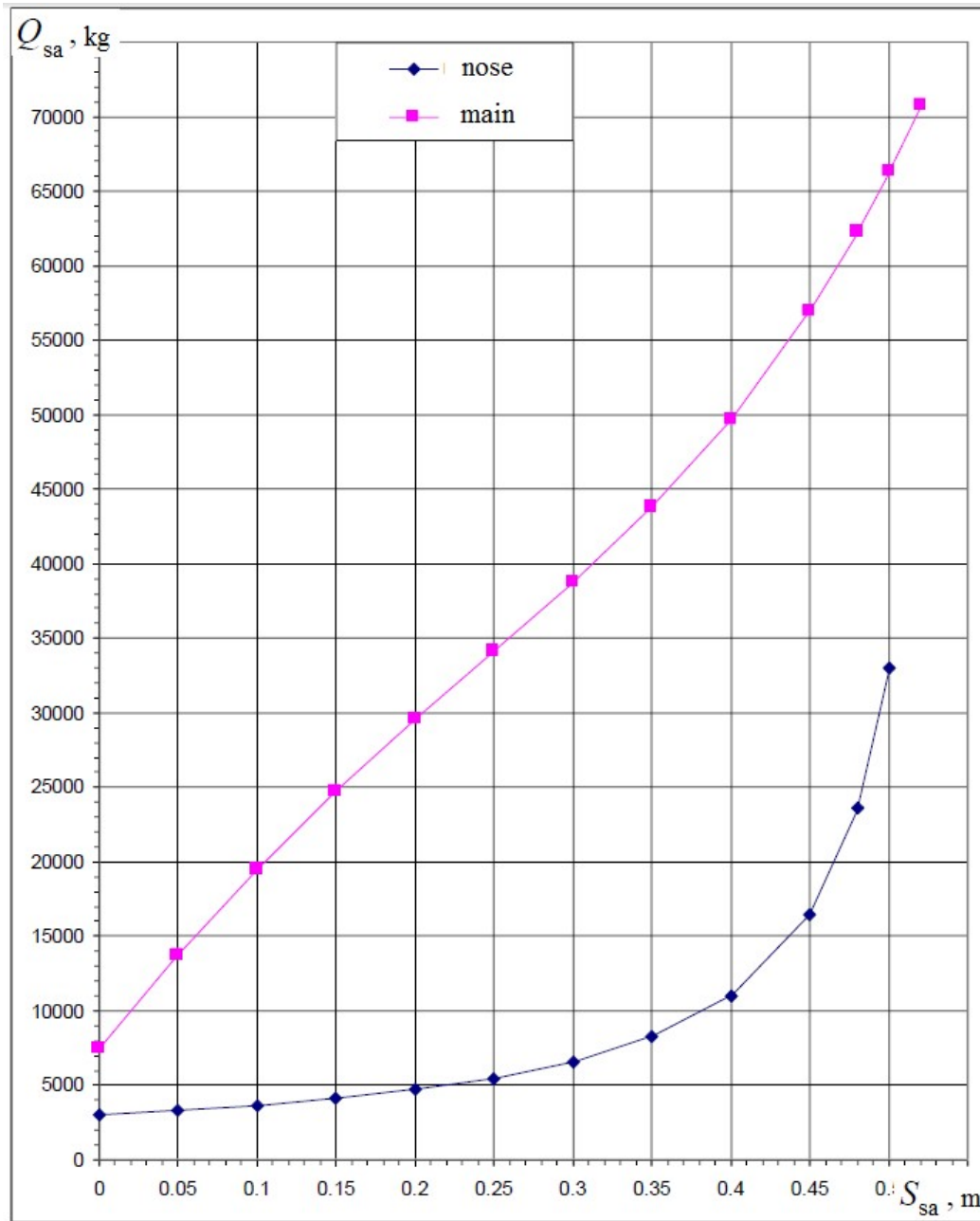


Figure 3-8: Diagram of shock absorbers

Related to directional control  $\mu_{z_0}^\beta$  derivative of side force on a wheel with respect to drift angle is assumed in the model in accordance with empirical dependence upon dimensionless load on a wheel  $\bar{p}_k$  as depicted on the next Figure 3-9:

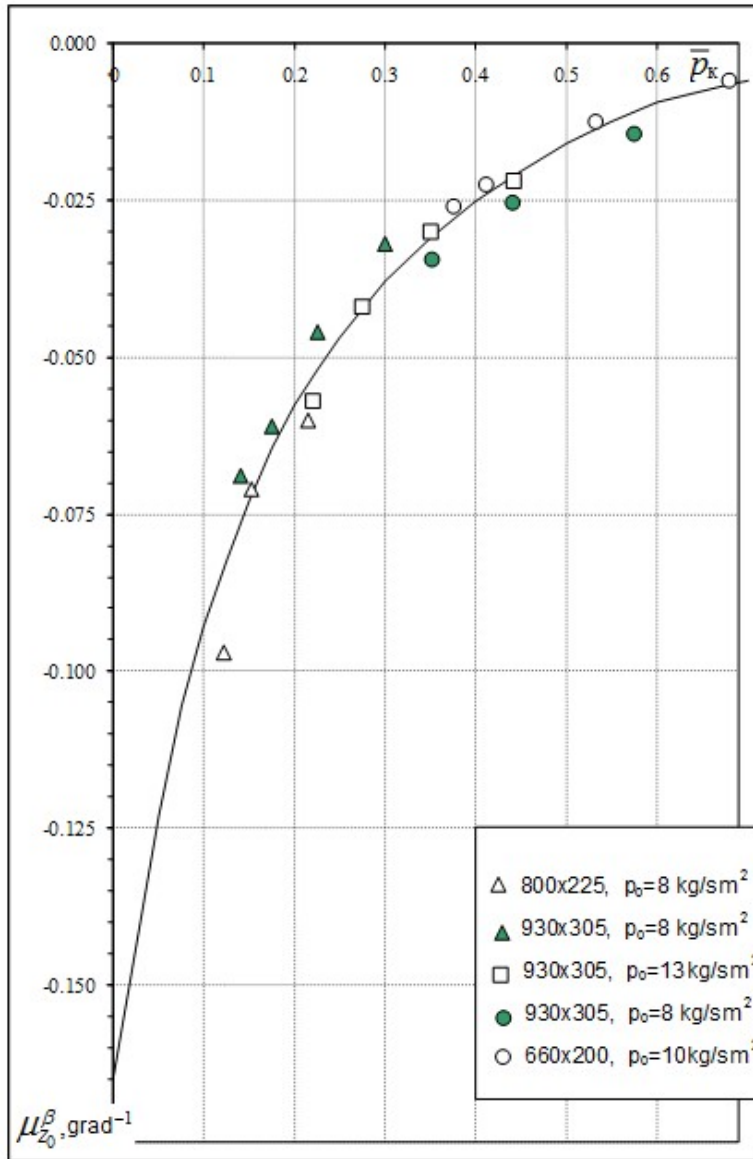
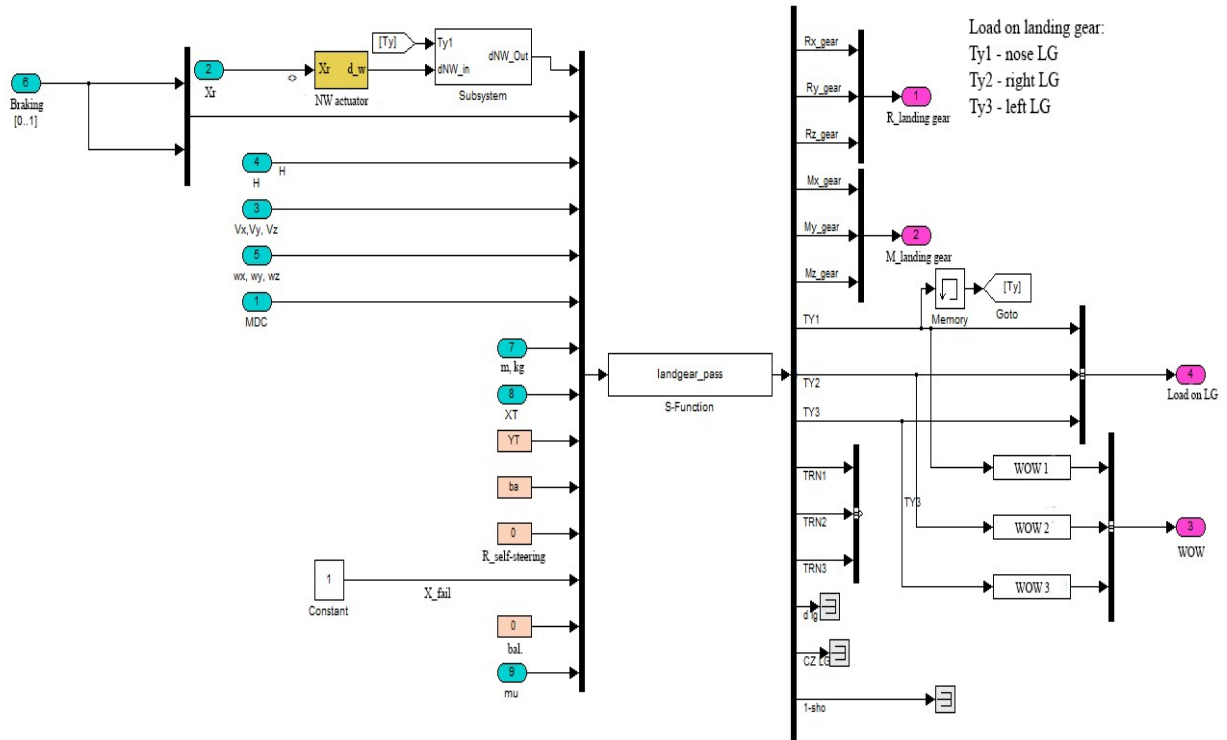


Figure 3-9:  $\mu_{z_0}^\beta$  versus  $\bar{p}_k$  dependency

There is used in calculation quasi-static model of braking (including anti-skid control).

### 3.2.3. Development of MATLAB/Simulink model of landing gear of typical commercial airliner

The Simulink diagram of this model is presented below in Figure 3-10. The main part of computations is executed by special S-function «landgear\_pass», which directly calculates all the forces and moments affecting aircraft by RUNWAY surfaces during ground run.



**Figure 3-10: Simulink diagram of the model of landing gear of typical commercial airliner**

#### Description of “landgear-pass” S-function.

This S-function contains the following inputs and outputs.

#### Inputs:

- nose wheel deflection,
- command signals of braking rate for left and right main landing gear legs,
- CG position above runway surface,
- 3 components of ground speed,
- 3 components of aircraft angular rate vector,
- matrix of direction cosines,
- weight of the aircraft,

- horizontal and vertical CG position,
- mean aerodynamic cord,
- flag of self-steering nose gear wheel,
- flag of engine failure,
- friction coefficient.

Outputs:

- 3 components for each force affecting the aircraft from runway surface,
- 3 components for each moments affecting the aircraft from runway surface,
- 3 vertical loads on each landing gear leg,
- 3 signs of compression of each landing gear leg,
- coefficients of rolling friction for the wheels of each landing gear leg,
- nose wheel deflection angle (for self-steering or for active control mode),
- side force coefficient for nose wheels,
- command signals for breaks pressure control.

### 3.3. Simulation of take off and landing run

For the time being absolutely predominant part takeoff and landing runs are fulfilled under pilot's control (except relatively little number of Cat. IIIb auto-landings). Thus, there is no availability to simulate these runs by utilizing mathematic methods only — it is necessary to use real pilot within the control loop. In other words there is inevitable need to put into practice engineering flight simulators with the pilot in the cockpit with all his capabilities and organically inherent limitations.

Naturally, indispensable condition of attaining acceptable result is adequate accuracy of mathematic model of aircraft motion on the ground. In accordance with TsAGI's opinion, up-to-date state-of-the-art in the area of such models, utilized in TsAGI and Russian aircraft design offices may be considered as satisfactory — there is accumulated positive experience of developing and validating the models, capable to support pilot-in-the-loop simulation for the purpose to certify adequately crosswind limitation under conditions of various RUNWAY contaminants. That is why this report is addressed to less investigated theme concerning the effect of simulator cockpit movability just from viewpoint of takeoff and landing run simulation.

#### 3.3.1. Analysis of contaminant type influence on the spectra of registered load factors

Correct representation of forces affecting the aircraft from runway surface covered by various contaminants is necessary for adequate representation of aircraft motion by flight simulators. In order to estimate the influence of contaminant type on spectra of load factor components registered on board there had been analyzed several landing records at the same RUNWAY of Khabarovsk airport under different whether conditions: 8 landing at clean and dry RUNWAY, 6 – at snow-covered runway, 1 – at water-covered runway and 1 – at runway be covered with ice.

All the analysis had been fulfilled in Matlab programming environment. Preliminary there had been performed interpolation of in-flight records by piecewise Hermitian polynomials with subsequent transformation of them to sampling frequency of 100Hz (this is operation frequency of flight simulator chosen by TsAGI's for this work). Then for all the cases under consideration the load factor components and rudder pedal deflection were drawn as time functions, and then corresponding spectral characteristics of them had been calculated.

One typical example of longitudinal load factor “ $n_x$ ” spectrum is presented below in Figure 3-11.

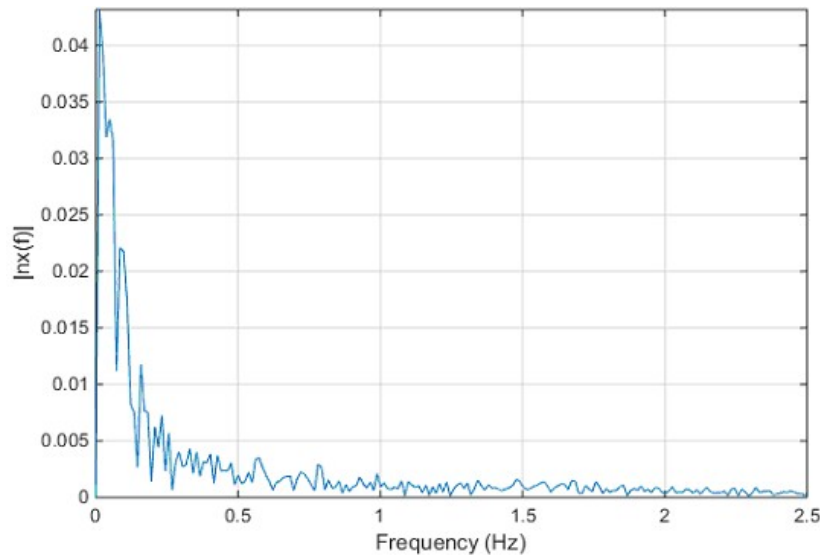


**Figure 3-11: The typical example of longitudinal load factor “ $n_x$ ” spectrum**

This spectrum and the spectra of other landings show that powerful low-frequency component dominates. So, creation of such low-frequency load factors is very important at flight simulators: it enables the pilot to evaluate deceleration rate of the aircraft and to form his judgment about runway contamination. As to high frequency part of spectrum, creation of it is not expedient because it is comparable with threshold level of pilot's perception and does not affect pilot's control. There had been revealed no significant difference among the properties of “longitudinal spectra” of all the landings considered.

One typical example of the spectra of lateral load factor “ $N_z$ ” and rudder pedals “ $X_H$ ” deflection is presented below in Figure 3-12. Unlike “longitudinal spectra” there exists in “ $N_z$ ” spectrum low-frequency component corresponding to the pilot's controls actions through rudder pedals deflections (and asymmetric breaking if utilized).

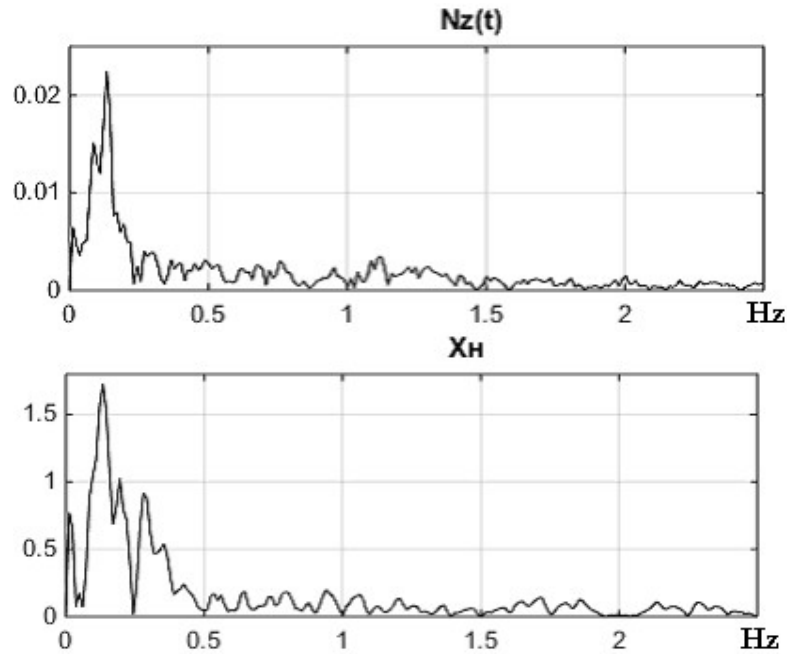


Figure 3-12: The typical example of lateral load factor “ $N_z$ ” and rudder pedals “ $X_H$ ” deflection spectra

Low-frequency part of spectrum is sufficiently perceptible for the pilots and helps them to recognize timely hazardous singularities of crosswise motion of the aircraft. So, creation of this part of spectrum at flight simulator is highly desirable.

The high-frequency magnitudes of “ $N_z$ ” surpass threshold level of pilot’s perception. But these frequencies are out of the bounds of pilot capability to control the aircraft. However, it is reasonable to create high-frequency “ $N_z$ ” to enhance pilot sensation of real flight.

### 3.3.2. Experiment arrangement

There are presented below in Figure 3-13, Figure 3-14 two photos illustrating design of flight simulator which was used in this work.



**Figure 3-13: Design of “PSPK-102” simulator**



**Figure 3-14: Interior of “PSPK-102” simulator cabin**

The simulator is equipped by both control columns and sidesticks.

Maximum values of available displacements, velocities and accelerations are presented in the following Table 3-1.

**Table 3-1: Maximum values of available displacements, velocities and accelerations**

	Displacements, m // deg	Velocities, mps // deg per s	Accelerations, Mps <sup>2</sup> // deg per s <sup>2</sup>
Longitudinal	±1.75	1.5	7
Vertical	±1.23	1.1	8
Lateral	±1.475	1.3	7
Bank	±35.1	30	230
Pitch	±37.8	30	230
Yaw	±60	50	260

Cockpit motion control laws are based on 3 widespread principles:

1. filtering low-frequencies components of accelerations,
2. diminishing the scales of their simulation,
3. using cockpit floor declining in simulation of longitudinal and lateral accelerations.

There are presented in the work standard control laws of the simulator that were also used in this work.

Specific control algorithm of cockpit motion (CACM) had been developed to meet the following requirements:

1. created accelerations should be as close to real as possible,
2. cockpit displacement commands should not to lead to attainment of physical limits,
3. spurious distortions of acceleration should be as low as possible.

For angular cockpit movements there had been used in such adjustment the requirement of the best coincidence of targeted (from aircraft movement model) and created (coming out the filters) angular rates. Naturally, the most attention in this work was paid to yaw motion, Figure 3-15:

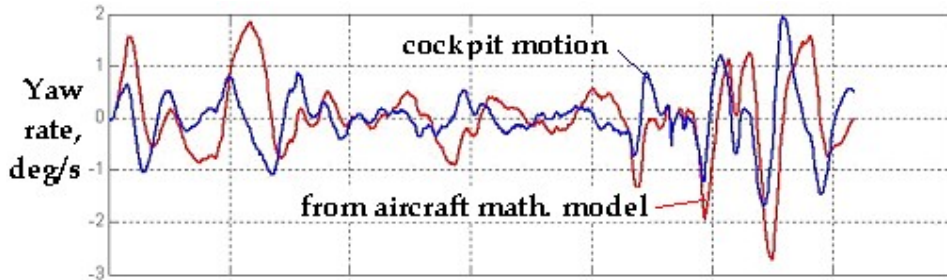


**Figure 3-15: Comparison of yaw angular rate variation in the cockpit and coming from mathematic model**

In order to meet aforementioned requirements and to provide availability to simulate all RUNWAY conditions and crosswinds, the parameters of the filters had been adjusted for the worst-case flight conditions leading to maximum cockpit displacements.

For the purpose to evaluate gain-phase distortions introduced by CACM there had been developed in TsAGI a few special criteria (with no relation to this work). As it is depicted on next Figure 3-16, at self-resonant (natural) frequencies of the filters in pitch and bank channels (“q” and “p” angular rates) quality is about 70%, and in yaw channel (“r” rate) it is close to 100%.

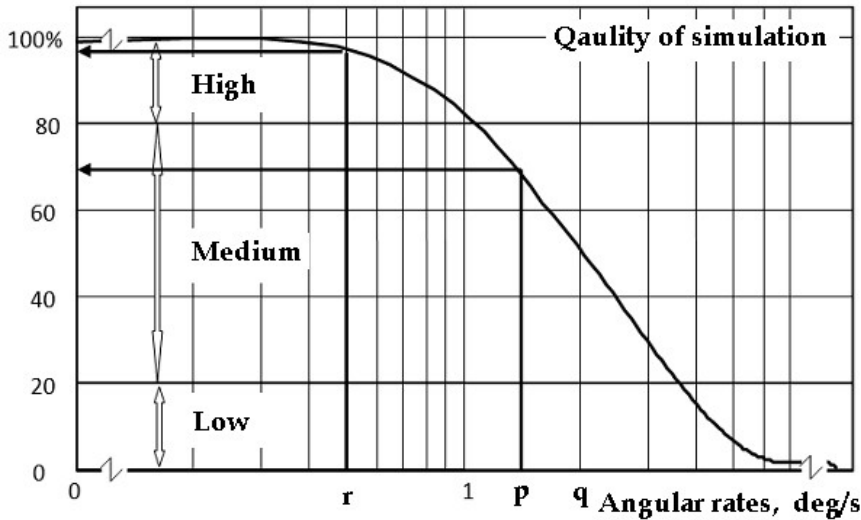


**Figure 3-16: Classification of “p”, “q”, “r” relative angular rate values**

As it is mentioned above, longitudinal load factor acts mainly at low frequencies. So, it is should be shaped through low-frequency filter controlling longitudinal slope of cockpit floor. The scale of representation was close to 1:1. Parameters of low-frequency filter had been selected with some reduction of representation scale. One example of coincidence of longitudinal load factor is presented in Figure 3-17:

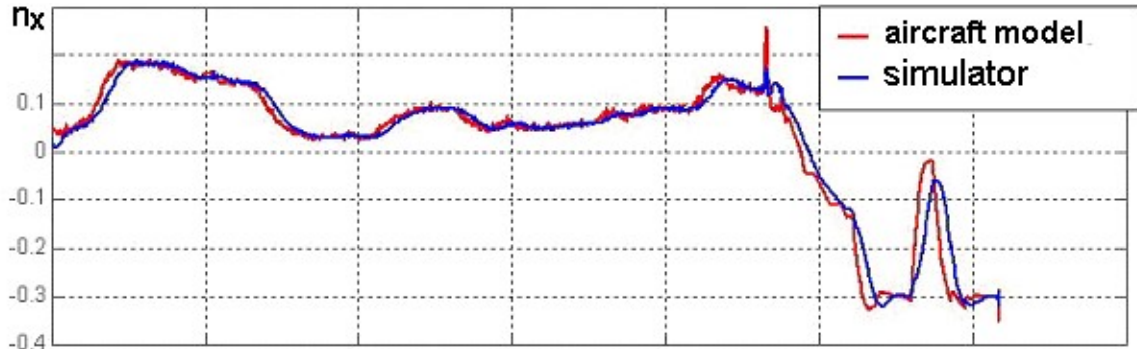


**Figure 3-17: The example of coincidence of longitudinal load factor**

Although lateral load factor “ $n_y$ ” is mainly also low-frequency and they are reproduced basically by low-frequency filters, 1:1 reproduction of “ $n_y$ ” is not expedient — it is known that variations of cockpit floor with frequency of 0.4...0.6 rad/s and magnitude in excess of 5 deg are perceive by the pilots just as angular motions of the cockpit, but not as linear motions of the aircraft. The parameters of low-frequency filter had been selected so that maximum lateral slopes of cockpit are not more than 2...4 deg, Figure 3-18:

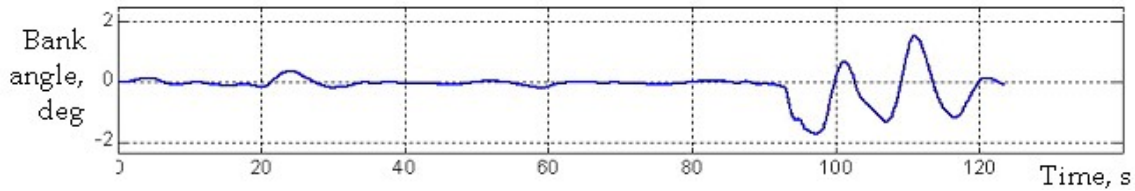


**Figure 3-18: Bank angle time history**

One example of coincidence of lateral load factor is presented below in Figure 3-19:

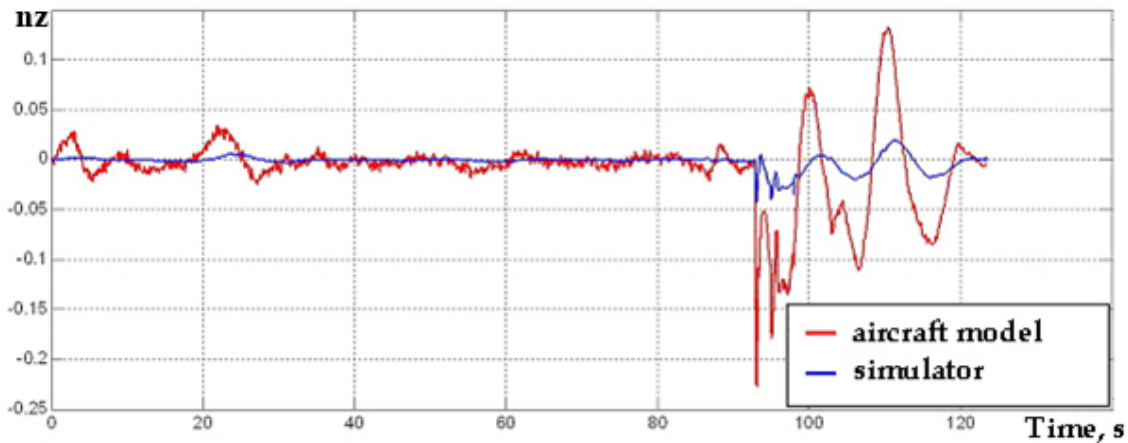


**Figure 3-19: Example of coincidence of lateral load factor**

There were simulated landings of typical commercial airliner under condition of constant crosswind (5 mps, 10 mps and 15 mps), Dryden’s turbulence of middle intensity (with root-mean-square [RMS] deviation of 1.5 mps) and various RUNWAY friction coefficients (0.6, 0.4 and 0.35). Initial point was at the distance of 2000 m from RUNWAY threshold with no bias from runway center line. Aircraft deceleration was done by using pilot’s pedals with no usage of thrust reversers.

The experiments were carried out with and without using of simulator movability. The aircraft was piloted by high skilled and experienced pilot. Totally, 77 landings had been fulfilled (including the landings to adjust all the parameters and simulator subsystems). And there had been carried out 26 valid trial to get the results. Alongside with subjective pilot’s comments there were obtained objective indicators of landing quality related to on-the-ground trajectory, RMS deviation of lateral load factor during landing run and others.

### 3.3.3. Analysis of the results

Next two plots Figure 3-20, Figure 3-21 demonstrate RMS deviations of lateral load factor “N<sub>z</sub>” with and without using of simulator movability.

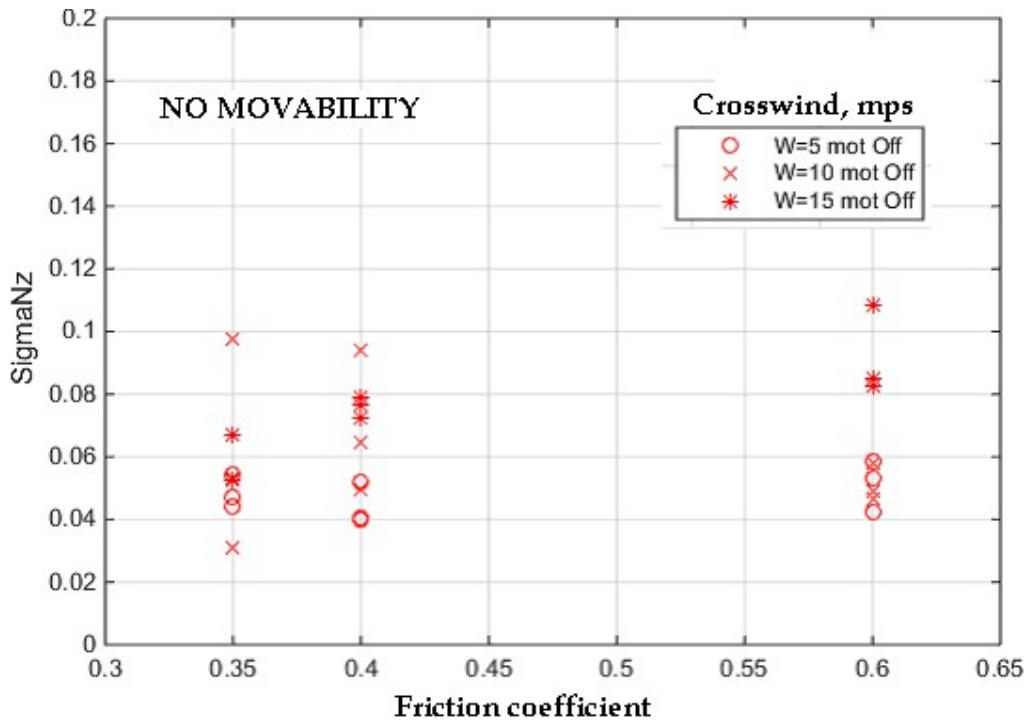


**Figure 3-20: RMS deviations of lateral load factor “N<sub>z</sub>” without using of simulator movability**

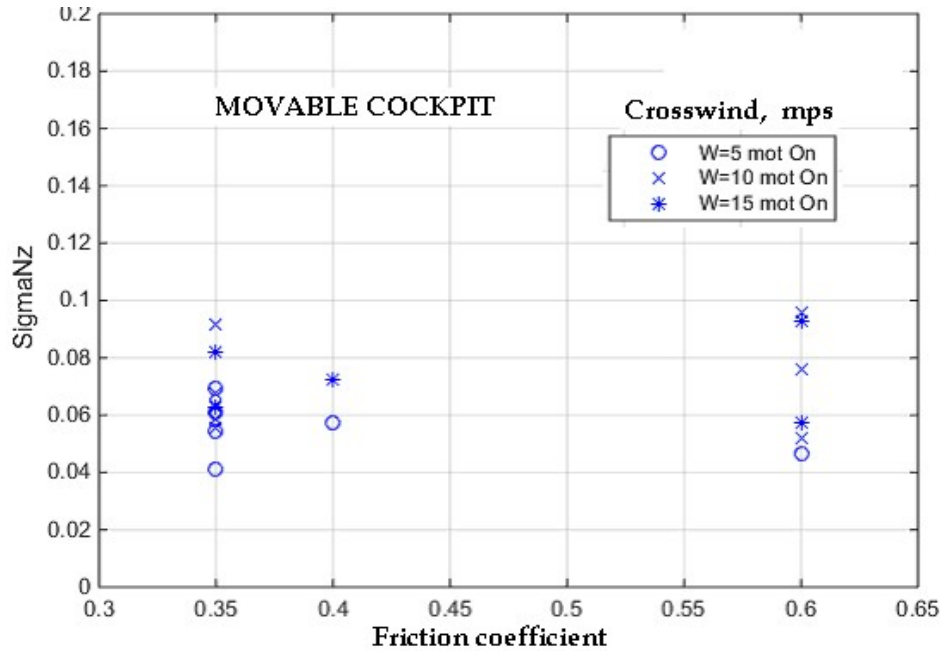


Figure 3-21: RMS deviations of lateral load factor "Nz" with using of simulator movability

It turns out that with movability both OFF and ON ("mot" on the next figure) lateral load factor depends on crosswind value: the more is crosswind, the more is load factor, Figure 3-22:

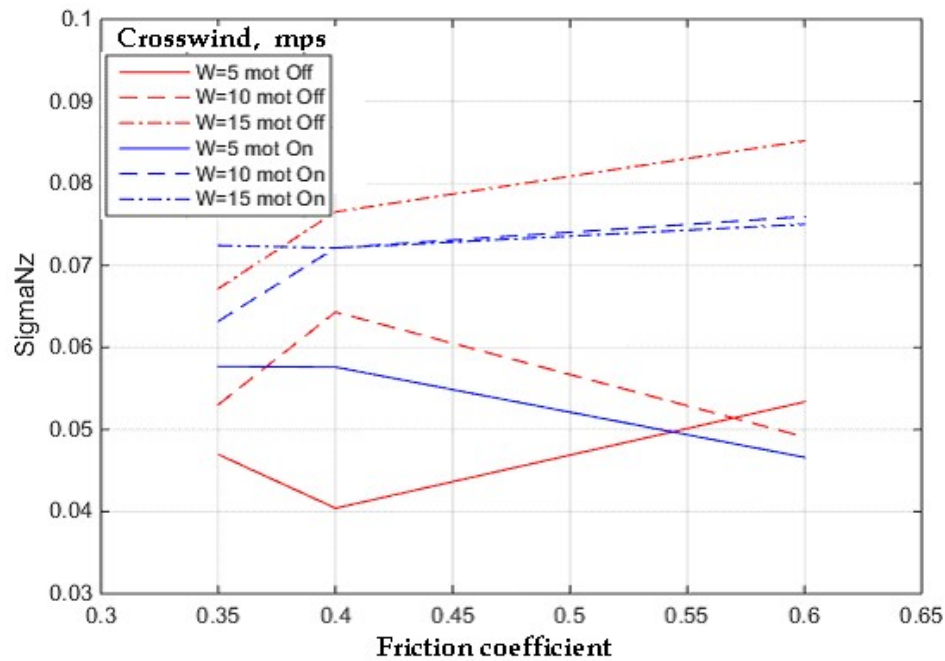


Figure 3-22: Dependency of lateral load factor on crosswind speed for various friction coefficients

Considerable difference in piloting characteristics and motion parameters had not been revealed. First, because of the relatively low frequency of on-the-ground trajectory control. Then, because pilot's control in this case is, in essence, "open-looped": the pilot controls the aircraft using mainly visual information, and feeling acceleration does not pass ahead of visual signs. However the pilot underlined that movability intensifies real flight feeling during landing run.

But movability effect seems to be significantly stronger under more complicated conditions of simulation:

- when friction coefficient depends on aircraft current position at runway,
- when friction coefficients are different for different landing gear legs,
- for soft contaminant at runway,
- for runway surfaces with significant irregularities,
- for complicated crosswind value behavior when it is changing during landing run.

### 3.4. Conclusions

There has been developed mathematical model of typical medium-sized civil airplane motion (both in the air and on the ground) enabling all-embracing simulation of approach and landing (as well as take-off) which calculates all the forces and moments caused by aerodynamics (including ground effect, high angles of attack and extremely high sideslip angles) and forces and moments generated by interaction of landing gear (LG) and RUNWAY surface. Among the other things this model takes also into calculation LG amortization, various levels of RUNWAY slipperiness and automatic deceleration functionality.

As it was cleared up by computational research, there exists no essential dependency of the spectrums of load factors during ground run on the type of RUNWAY contaminant.

Pilot-in-the-loop simulation of landing with using simulator with movable cockpit reveals no dependence of pilot's control quality and accuracy on presence or absence of movability.

## 4 CONCLUSIONS AND RECOMMENDATIONS

Firstly, this study analysed the potential impact that shortcomings in existing models have on guidance material (crosswind limits) provided by aircraft manufacturers. The results from the simulator experiments and fast-time simulations show that there is a significant difference between the maximum crosswind that is considered acceptable by pilots in terms of controllability demands and the crosswind that actually exceeds the capacity of the aircraft to counter the side forces generated by the crosswind in the landing roll. The first leads to significantly lower crosswind limits and is the primary factor in the determination of these limits. Because the workload for pilots cannot be assessed in fast-time simulations, simulator experiments are essential. While turbulence seems to have little effect on the crosswind at which the aircraft loses the ability to generate the required side forces to retain directional control in the ground roll, it does have a major impact on the control efforts required by the pilot, especially in the airborne phase. It is therefore essential that turbulence is included in simulator experiments aimed at determining crosswind limits. The fast-time simulations show that the level of sophistication of the landing gear model has an impact on the assessment of crosswind limits. The landing gear model should at least account for the interaction between side and braking friction. Standard landing gear models like the Fokker 100 model account for these effects. Using even more sophisticated models that more accurately reflect the high frequency dynamics of the landing gear at touchdown and wheel spin-up may lead to more realistic ground reaction forces. But as the crosswind limits are mainly determined by the pilot workload in controlling the aircraft, the benefit of using such models is questionable. When a standard landing gear model is used, a basic update rate (100Hz) is sufficient. Finally, it is noted that, due to a lack of test data, the accuracy of aerodynamic models in low speed and/or high sideslip conditions is questionable. This may have a significant impact on the fidelity of simulations to assess crosswind limits. This potential shortcoming could not be assessed in this study, but is further addressed in a separate activity in Future Sky Safety.

Next, the significance of providing load factors information from viewpoint of accuracy of pilot-in-the-loop simulation was investigated. There has been developed mathematical model of typical medium-sized civil airplane motion (both in the air and on the ground) enabling all-embracing simulation of approach and landing (as well as take-off) which calculates all the forces and moments caused by aerodynamics (including ground effect, high angles of attack and extremely high sideslip angles) and forces and moments generated by interaction of landing gear (LG) and runway surface. Among the other things this model takes also into calculation LG amortization, various levels of runway slipperiness and automatic deceleration functionality. As it was cleared up by computational research, there exists no essential dependency of the spectrums of load factors during ground run on the type of runway contaminant. Pilot-in-the-loop simulation of landing with using simulator with movable cockpit reveals no dependence of pilot's control quality and accuracy on presence or absence of movability.

## 5 REFERENCES

1. Shortcomings in current modelling for modern aircraft, FSS\_P3\_NLR\_D3.2, H.T.H. van der Zee, 22-02-2016.
2. Aerodynamic data of the Fokker 100, L-28-336, issue no 8.61, Fokker Aircraft B.V., May 1995.
3. Non-aerodynamic data related to the Fokker 100 aero database, L-28-586, issue no 1, Fokker Aircraft B.V., January 1995.
4. Aircraft on Ground Performance, Boeing Report D6-44062.
5. GRACE - a Versatile Simulator Architecture Making Simulation of Multiple Complex Aircraft Simple, W.W.M. Heesbeen, R.C.J. Ruigrok, J.M. Hoekstra, AIAA MST Conference and Exhibit, August 2006.
6. The use of pilot rating in the evaluation of aircraft handling qualities, NASA TN D-5153, G.E. Cooper & R.P. Harper, April 1969.
7. Boeing 747 Pilot Control Model for the Balked Landing, NLR-CR-2011-063, P.J. van der Geest & H.T.H. van der Zee, November 2011.
8. Validation of aircraft simulation models for the analysis of in-trail following dynamics - Deliverable D1 of the AMAAI project, NLR-CR-2002-044, P.J. van der Geest, January 2002.
9. Aircraft Operations Manual Fokker 70/100, 22 December 2005.
10. EASA Certification Specifications for All Weather Operations (CS-AWO), 17-10-2003.
11. 1. V.F. Bragazin. Stability and controllability of aircraft motion at runway. Encyclopedia of engineering. Vol. IV-21 "Aerodynamics, flight dynamics and strength of flying vehicles." Book 1. Mechanical engineering. Moscow, 2002.
12. O.E. Lopanitsyn, V.V. Strelkov, E.E. Utkina. "Development of a ground effect math model for flight dynamics problems based on two-parameter approximation of wind tunnel data." Aeronautical Engineering (TVF) # 2 (685), 2007.
13. L.E. Zaichik, V.V. Rodchenko, Y.P. Yashin, I.V. Rufov, A.D. White. "Acceleration perception", AIAA-99-4334, Portland OR, 1999.
14. V.V. Rodchenko, A.D. White, "Motion Fidelity Criteria Based on Human Perception and Performance," AIAA-99-4330, Portland OR, 1999.
15. L.E. Zaichik, V.V. Rodchenko, Y.P. Yashin, B.P. Lee. Simulation-to-flight correlation. AIAA-2003-5823, AIAA MST Conference, Texas, 2003.
16. L.E. Zaichik, Y.P. Yashin, P.A. Desyatnik, "Motion Fidelity Criteria for Large-Amplitude Tasks", AIAA-2009-5916, Chicago II, 2009.
17. L.E. Zaichik, Y.P. Yashin, P.A. Desyatnik, "Peculiarities of Motion Cueing for Precision Control Tasks and Maneuvers," ICAS Paper 602, Nice, France, 2010.
18. Approach and Landing Accident reduction (ALAR tool kit). Flight safety foundation. 2013.
19. Runway excursions, Part 1. A worldwide review of commercial jet aircraft runway excursions. Aviation Research and analysis report. Australian transport safety bureau. AR-2008-018(1), 2008.
20. G. van Es. Excursions from European perspective: mitigating measures and preventing actions. NLR/Eurocontrol, 2010.

21. G. van Es. Safety aspects of aircraft performance on wet and contaminated runways. Flight Safety foundation 10-th annual European aviation safety seminar, Amsterdam, March 1998.
22. G.W.H van Es, P.J. van der Geest, T.M.H. Nieuwpoort. Safety Aspects of aircraft operations in crosswind. NLR-TP-2001-217.
23. A.P. Yuzokas, G.D. Savikov and others. Investigation and analysis of incidences occurred in 2011 and related to RUNWAY excursions of civil aviation aircrafts during landing. Development of additional recommendation for the pilots and training staff focused on prevention of excursions. Description of the most serious events. Report of State Center "Flight safety in civil aviation", 2012.
24. Takeoff and landing Performance assessment validation efforts of runway conditions assessment matrix (RCAM). DOT/FAA/TC-TN13/22, 2013.
25. Varyukhina E.V., Pavlov A.A., Strelkov V.V., Luchinin V.V. Analysis of contributory risk factors in runway excursions and method of difficulty assessment. . The 11-th International Exhibition and Scientific Conference on Hydroaviation GELENDZHIK-2016, 22-25 September, 2016
26. V.V. Strelkov. TsAGI research aimed at mitigating of runway excursions. ICAO EUR Regional Safety Team ninth meeting. Tbilisi, Georgia, 13-15 June 2017.
27. V.V. Strelkov, D.V. Razumov, M.N. Zuev and others. "RRJ-Express" Special Software for Flight Data Processing." SW License #2011614481 dated from 2011. Russian Federal Service for Intellectual Property (Rospatent).
28. Y.V. Burov, V.V. Strelkov. Software for decoding raw data from quick access recorder of passenger aircraft "ARINC-converter". SW License #2016662052 dated from 2016. Russian Federal Service for Intellectual Property (Rospatent).
29. Global Positioning System Standard Positioning Service Performance Standard (GPS SPS PS). 4th Edition. September 2008.
30. G. de Rivals. Flight Operations Analysis. Landing Trajectory Computation. EOFDM 3rd conference. February 2014
31. Lin J., Keogh E., Lonardi S., Chiu B. A Symbolic Representation of Time Series, with Implications for Streaming Algorithms. In Proceedings of the 8th ACM SIGMOD Workshop on Research Issues in Data Mining and Knowledge Discovery (DMKD '03), San Diego, CA, USA, 13 June 2003; pp. 2–11.
32. Keogh E., Chakrabarti K., Pazzani M., Mehrotra S. Dimensionality Reduction for Fast Similarity Search in Large Time Series Databases. Knowledge and Information Systems (2001) 3: 263. doi:10.1007/PL00011669.
33. J. Zhang and H. Wang. Detecting outlying subspaces for high-dimensional data: the new task, algorithms, and performance. Knowledge and information systems, 10(3):333–355, 2006.
34. M. Breunig, H. Kriegel, R. Ng, and J. Sander. LOF: identifying density-based local outliers. In Proceedings of the ACM SIGMOD International Conference on Management of Data, volume 29, pages 93–104. ACM, 2000.
35. A. Srivastava. Enabling the discovery of recurring anomalies in aerospace problem reports using high-dimensional clustering techniques. In Proceedings of the IEEE Aerospace Conference, 2006, pages 1–17. IEEE, 2006.

36. M. Augusteijn and B. Folkert. Neural network classification and novelty detection. *International Journal of Remote Sensing*, 23(14):2891–2902, 2002.
37. S. Hawkins, H. He, G. Williams, and R. Baxter. Outlier detection using replicator neural networks. In *Data warehousing and knowledge discovery*, volume 2454, pages 113–123. Springer, 2002.
38. L. Li et al. Anomaly detection via Gaussian Mixture Model for flight operation and safety monitoring. *Transportation Research Part C: Emerging Technologies*. Volume 64, March 2016, Pages 45-57. <https://doi.org/10.1016/j.trc.2016.01.007>.
39. Mann H. B., Whitney D. R. On a test of whether one of two random variables is stochastically larger than the other. // *Annals of Mathematical Statistics*. — 1947. — № 18. — P. 50–60.
40. Benjamini, Y. (1988). "Opening the Box of a Boxplot". *The American Statistician*. 42 (4): 257–262. doi:10.2307/2685133. JSTOR 2685133.
41. Myers, Jerome L.; Well, Arnold D. *Research Design and Statistical Analysis* (2nd ed.). Lawrence Erlbaum. p. 508, 2003.